博士学位論文

Dissertation

Doctoral

Study on facile fabrication of super strong cellulose hydrogel with anisotropic hierarchical fibrous structure

異方的階層繊維構造を持つ超高強度セルロースハイドロゲルの簡便な製造に関する研究

by

郭 雲 舟

Guo,YunZhou

Supervisor

Professor. Jian Ping Gong

北海道大学大学院生命科学院

Graduate School of Life Science, Hokkaido University

2021 年 12 月

December 2021

CHAPTER 1

General Introduction

1.1 Overview

Natural structural materials are built at ambient temperature from a fairly limited selection of components. They usually comprise hard and soft phases arranged in complex hierarchical architectures, with characteristic dimensions spanning from the nanoscale to the macroscale. [1] The resulting materials are lightweight and often display unique combinations of strength and toughness. With the unique mechanical performance, natural structural materials like tendon, ligaments and bones can provide essential support for all kinds of functions. The early technological development of humanity was supported in its early stages by natural materials such as bones, wood and shells.[2] As history advanced, these materials were slowly replaced by synthetic compounds that offered improved performance. Today, scientists and engineers continue to be fascinated by the distinctive qualities of the elegant and complex architectures of natural structures, which can be lightweight and offer combinations of mechanical properties that often surpass those of their components by orders of magnitude. Contemporary characterization and modelling tools now allow us to begin deciphering the intricate interplay of mechanisms acting at different scales — from the atomic to the macroscopic — and that endow natural structures with their unique properties. At present, there is a pressing need for new lightweight structural materials that are able to support more efficient technologies that serve a variety of strategic fields, such as

transportation, buildings, and energy storage and conversion. [ref] To address this challenge, yet-to-be-developed materials that would offer unprecedented combinations of stiffness, strength and toughness at low density, would need to be fashioned into bulk complex shapes and manufactured at high volume and low cost.

Hydrogels are formed through the cross-linking of hydrophilic polymer chains within an aqueous microenvironment, the water rich nature of hydrogels makes them broadly applicable to many areas, including tissue engineering, drug delivery, soft electronics, and actuators. [3] Conventional hydrogels usually possess limited mechanical strength and are prone to permanent breakage. The lack of desired dynamic cues and structural complexity within the hydrogels has further limited their functions. Broadened applications of hydrogels, however, require advanced engineering of parameters such as mechanics and spatiotemporal presentation of active or bioactive moieties, as well as manipulation of multiscale shape, structure, and architecture.

Inspired by nature biological materials, many methods have been developed to make polymer fibers in dry or hydrogel form including wet/melt spinning, electrospinning, and microfluidic techniques, where polymer solutions or melts are drawn as fibers with diameters on the order of micrometers to sub-micrometers.[4] But constructing an anisotropic bulk hydrogel containing biomimetic hierarchical fibrous architecture is still a challenge. In the previous work, we developed a facile method called Drying in Confined Condition method, simple as DCC method, [5] through which we successfully fabricated anisotropic alginate hydrogels with hierarchical fibrous architectures. Besides the biomimetic structure, the alginate

hydrogels also exhibit mechanical properties similar to those of load bearing natural tissues such as ligaments and tendons.

1.2 Outline of this dissertation

It's been widely studied that the extreme mechanical property of connective tissues like tendon and ligaments result from the highly aligned and hierarchical fibrous structure. Besides the extreme strength, the toughness of those connective tissues are also excellent. Preparation of finely organized fibrous structure which can optimize the strength and toughness is really challenging for hydrogel scientists.

Previously, our lab developed a facile method called Drying in Confined Condition method, simple as DCC method, which can effectively produce highly aligned and hierarchical fibrous structure on alginate hydrogels, the resulting strength can reach the human ligaments level, but the extreme strength of achilles tendon (~80MPa) is still far from reaching. And since alginate hydrogel is not stable in saline solution due ionic cross-linking, which would limit the application prospect.

Hence in this study, we choose cellulose as raw material, and focus on preparation of super strong cellulose hydrogel through DCC method. We successfully improved the mechanical strength of purely cellulose based hydrogel to human achilles tendon level, and meanwhile there is no sacrificing in toughness. Through multiple characterization method, we confirmed the high orientation degree through different scales and the way of fibrils aggregation play important role in the improved mechanical performance.

In chapter 1, general introduction and outline of the dissertation are discussed.

In chapter 2, a brief review on the strong and tough hydrogels, strengthen and toughening strategies are introduced. Meanwhile, brief introduction on the DCC method and the validity of this method are discussed. The effect of DCC method on different polymers are compared.

In chapter 3, the ideal environmental condition on preparation of DCC-Cellulose hydrogels are discussed.

In chapter 4, extremely strong and purely cellulose-based cellulose gels are prepared, The high strength and toughness of the DCC-E gels were realized by optimizing the cellulose fibril arrangement from nanoscale to macroscale, which was done by selection of an appropriate solvent used for cellulose regeneration. Parallel aggregated fibrous structures observed in the DCC-E gels are thought to play a central role in the enhancement of both toughness and strength.

In chapter 5, the toughening mechanism of DCC-Cellulose hydrogel have been explored through SEM and cycling tests. It's been clarified that untwisting of hierarchical fibrous structure under loading is the main mechanism for energy dissipation. And abundant hydrophobic interaction between fibrous structure have been confirmed through immersing the samples in urea solution to observation the change of fibrous structure and compare the hysteresis change in cycling tests.

In chapter 6, by using DCC process as training method, we successfully further improved the mechanical property of cellulose hydrogel. By various characterization, we confirmed that during repetitive DCC process, cellulose fibrils become more aggregated together. And by

giving a extreme pretrain in the second DCC process, we find the fracture stress is hard to breakthrough 90 MPa.

In chapter 7, conclusions of the dissertation are summarized.

1.3 References

[1] Peter Fratzl, Richard Weinkamer, Nature's hierarchical materials, *Progress in Materials Science*, 52, 8, 2007, 1263-1334, https://doi.org/10.1016/j.pmatsci.2007.06.001.

[2] Marc André Meyers, Po-Yu Chen, Albert Yu-Min Lin, Yasuaki Seki, Biological materials: Structure and mechanical properties, *Progress in Materials Science*, 53, 1, 2008, 1-206, https://doi.org/10.1016/j.pmatsci.2007.05.002

[3] Y. S. Zhang, Ali. Khademhosseini, 2017. Advances in Engineering Hydrogels. Science. 356, eaaf3627. https://doi.org/10.1126/science.aaf3627

[4] Shuming Zhang, Xi Liu, Sebastian F. Barreto-Ortiz, Yixuan Yu, Brian P. Ginn, Nicholas A. DeSantis, Daphne L. Hutton, Warren L. Grayson, Fu-Zhai Cui, Brian A. Korgel, Sharon Gerecht, Hai-Quan Mao, Creating polymer hydrogel microfibres with internal alignment via electrical and mechanical stretching, *Biomaterials*, 35, 10, 2014, 3243-3251, https://doi.org/10.1016/j.biomaterials.2013.12.081.

[5] M. T. I. Mredha, Y. Z. Guo, T. Nonoyama, T. Nakajima, T. Kurokawa, J. P. Gong, A Facile Method to Fabricate Anisotropic Hydrogels with Perfectly Aligned Hierarchical Fibrous Structures. Adv. Mater. 30 (9) (2018) 1704937. https://doi.org/10.1002/adma.201704937

CHAPTER 2

Background

2.1 DCC method

Our facile method includes drying a piece of diluted physical hydrogel consisting of semi rigid/rigid polymers in air at a confining geometry, as shown in Figure 2.1(I). This drying in confined condition method is abbreviated DCC. During drying, the gel shrinks due to the evaporation of water (Figure 2.1(II)). As its two ends are fixed, the width and thickness of the hydrogel will shrink, but not the length. Therefore, the gel experiences tensile stress in the length direction during drying, causing orientation of the polymer chains along the length direction. When dried, the polymer concentration increases and above a critical concentration the polymers form nanofibrils through supramolecular interactions (Figure 1(II)). Further drying induces aggregation of nanofibrils to form thicker fibers. The process is repeated to form the hierarchical fibrous structure of the gel (Figure 1(III)). The reswollen gel maintains the same structure due to the formation of stable supramolecular interactions (Figure 2.1(IV)).

Different rigid/semi-rigid linear polysaccharides such as alginate, cellulose, and chitin are critical to the morphogenesis and functionality of various hierarchically ordered natural materials.[1]

2.2 DCC method on various polymer hydrogels.

To confirm the effect of DCC method on different biopolymers, we applied DCC method on cellulose hydrogel, alginate hydrogel and chitin hydrogel respectively. Cellulose and chitin

hydrogel are cross-linked through purely physical interaction like hydrogen bonding and hydrophobic interaction, alginate hydrogel has Ca2+ ion as ionic crosslinking. As shown in Figure 2.2, The SEM results show rather different morphology depending on the type of biopolymers, cellulose hydrogel shows a twistedly aggregated fibrous structure, alginate hydrogel shows parallelly aggregated fibrous structure, and chitin hydrogels show blurred fibrous structure. Hence cellulose and alginate are better choices for preparing biomimetic fibrous structure. For further comparison, we tested the mechanical performance of DCC-cellulose hydrogel and DCC-alginate hydrogel, elaborate results are listed in table 2.1, as the results show, DCC-Cellulose hydrogel are stronger than the corresponding DCC-alginate hydrogel. The young's modulus and fracture stress of DCC alginate hydrogel with 50% prestrain shows high young's modulus(~370MPa) and fracture stress(~20MPa), but this is still far from the mechanical performance of human achilles tendon. The mechanical property of hydrogel needs to be further improved to serve the requirements in more emerging areas. And we further tried subcutaneous implantation of different DCC samples to the back of rabbit, to check the biocompatibility of those samples. As show in Figure 2.3, after 2 weeks of implantation, only DCC-Cellulose hydrogel shows no obvious degradation and inflammation. Considering the possible application in tissue engineering, materials possess both good mechanical and biological property will be the first choice, hence we choose to use cellulose as the material to further enhance the mechanical property and elucidate the fibrous structure.

2.3 References

[1] M. T. I. Mredha, Y. Z. Guo, T. Nonoyama, T. Nakajima, T. Kurokawa, J. P. Gong, A Facile Method to Fabricate Anisotropic Hydrogels with Perfectly Aligned Hierarchical Fibrous Structures. Adv. Mater. 30 (9) (2018) 1704937. https://doi.org/10.1002/adma.201704937

2.4 Figures

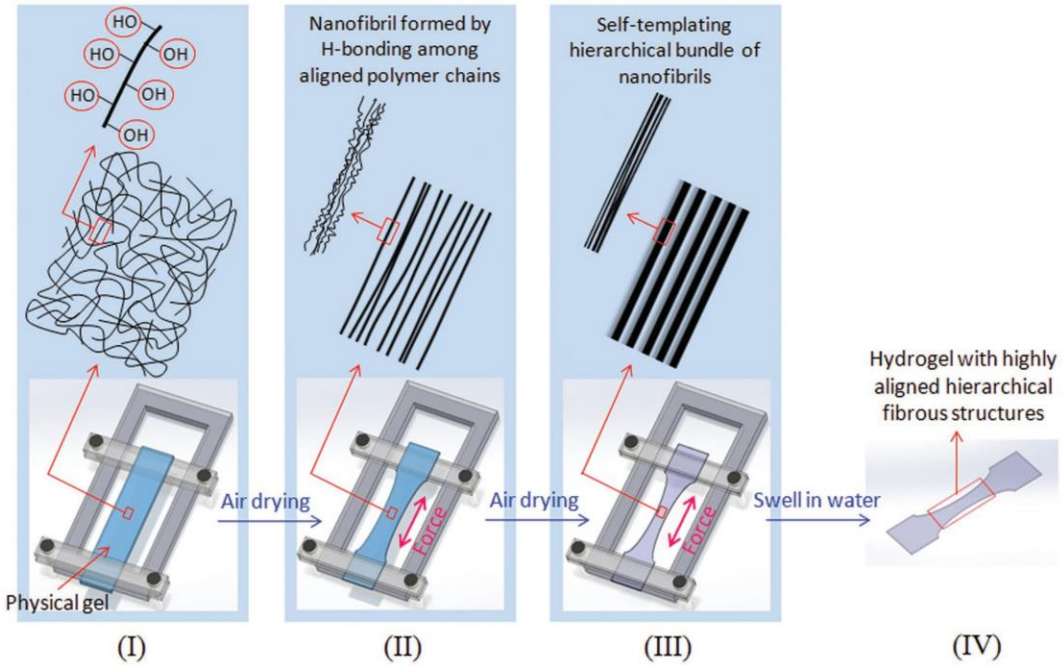

Figure 2.1 Design strategy. Schematic illustrations of DCC (drying in confned condition) method for creating perfectly aligned fbrous hydrogels with hierarchical superstructures. A rectangular piece of physical hydrogel (having fber-forming H-bonding sites) is clamped to a sample holder at its two long ends (I). The gel is left to dry in air. Due to volume contraction during the drying process, the gel's width and thickness shrink. As the shrinking in the length direction is restricted by the sample holder, the gel experiences tension along the length

direction, which aligns the polymer chains in the length direction. When polymer density reaches the fber forming concentration by drying, thin fbrils are formed along the tensile direction through H-bond formation (II). Further drying induces aggregation of nanofibrils to form thick fibers; this process is repeated to form the hierarchical fibrous structure of the gel (III). The reswollen gel maintains the same structure due to the formation of stable H-bonds (IV). [REF]

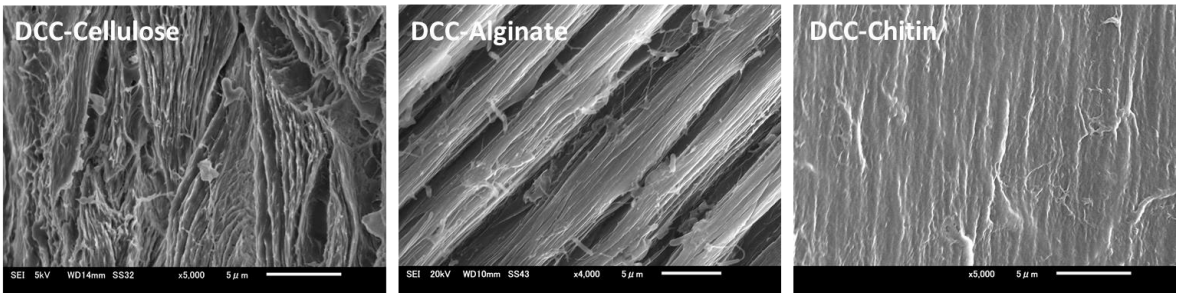

Figure 2.2 SEM photo showing the surface morphology of DCC-Cellulose, DCC-Alginate and DCC-Chitin respectively.

Table 2.1 Mechanical properties and water contents of hydrogels prepared under different conditions. All the properties were measured after reswelling in water. Data are presented as average value with standard deviation from three measurements. Data are compared with human knee ligaments.

Hydrogel name	Sample description	Young's modulus, E [MPa]	Fracture stress, σ_f [MPa]	Fracture strain, ε_f [%]	Work of extension, W [MJ m^{-3}]	Water [wt%]
Ca-alginate	Initial swollen sample	0.39 ± 0.05	0.32 ± 0.03	145.9 ± 23.3	0.24 ± 0.05	95
ND-alginate	Free dried	64.02 ± 14.35	10.26 ± 1.76	178.4 ± 14.7	11.78 ± 2.79	56
DCC-alginate	DCC without prestretching[a)]	203.3 ± 14.33	22.43 ± 0.93	201.4 ± 15.9	30.88 ± 1.97	57
50%DCC-alginate	DCC at 50% prestretching	367.35 ± 54.49	19.80 ± 2.24	51.1 ± 2.5	7.04 ± 0.45	56
p-Cellulose	Initial swollen sample	2.49 ± 0.21	1.58 ± 0.09	204.8 ± 11.0	1.48 ± 0.14	88
ND-cellulose	Free dried	19.20 ± 0.89	12.62 ± 0.40	407.7 ± 34.9	20.62 ± 2.18	59
DCC-cellulose	DCC without prestretching	59.0 ± 6.57	25.80 ± 1.33	267.3 ± 1.3	38.03 ± 2.83	58
50%DCC-cellulose	DCC at 50% prestretching	150.67 ± 11.79	39.33 ± 7.31	102.2 ± 9.0	32.04 ± 1.75	58
100%DCC-cellulose	DCC at 100% prestretching	342.44 ± 31.14	53.55 ± 0.53	34.7 ± 6.4	16.44 ± 0.99	58
Knee ligaments[b)]	–	65–447	13–46	11–44	–	60–70

a)DCC: drying in confned condition; b)Human knee ligament data from medial collateral ligament (MCL), anterior cruciate ligament (ACL), and posterior cruciate ligament (PCL) are shown.[17,18]

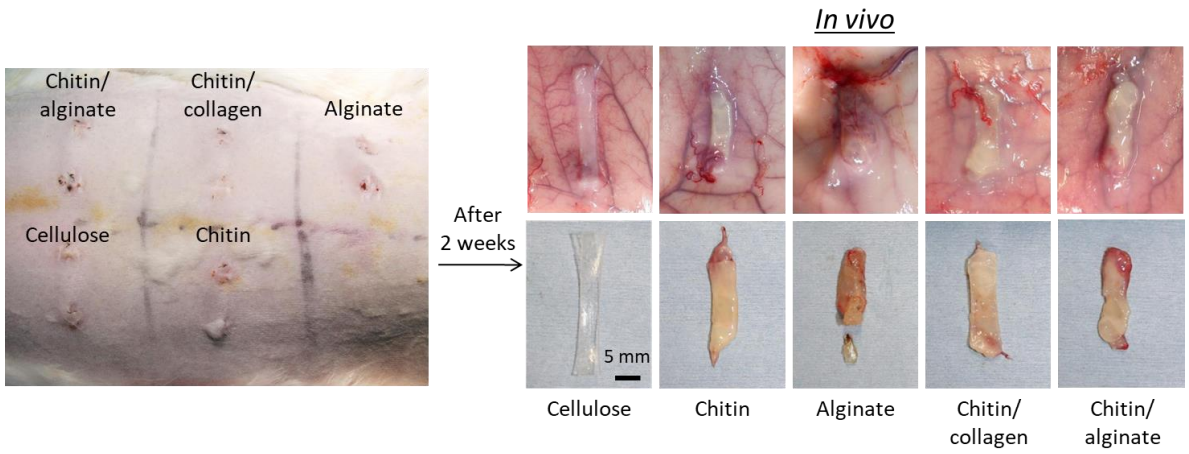

Figure 2.3 In vivo tests of various DCC biopolymer hydrogels. Subcutaneous implantation to the back of the rabbit to check the biocompatibility of different DCC biopolymer hydrogels.

CHAPTER 3

Exploring the environmental effect on structure and performance of DCC-Cellulose hydrogel.

3.1 Introduction

In our previous work, we developed a facile method, called Drying in Confined Condition method, simple as DCC method, through which we produced DCC-alginate hydrogels with highly aligned hierarchical fibrous structure. [1] This highly biomimetic structure improved the mechanical performance of alginate hydrogel to the level of some connective tissues in human body, for example, ligaments.

But as we mentioned in chapter 2, alginate hydrogel is instable under saline solution due the ionic crosslinking of Ca2+ ions. For application in the field of bio-engineering, a chemically stable biopolymer would be the best candidate. And hopefully can give a better mechanical performance to the final sample so that all of the connective tissues could be covered for future medical application.

With above consideration, we choose cellulose gel for DCC method, because cellulose molecules aggregate through hydrogen bonding and hydrophobic interaction, [2] which is a solid foundation for the chemical stability under saline solution. And most materials made of cellulose are famous for the high strength. Another advantage of cellulose is the vast source from the nature, cellulose is most abundant biopolymer in the world, with development of process techniques, cellulose can be easily refined and processed into ideal state like cellulose nanofibrils, cellulose nanocrystals, for application in a variety of areas, especially the biomedical areas.

So in the first place, we need to confirm the optimal environmental conditions during the process of preparation of original gels and the DCC method. Based on the results, we will be able to further explore the possibility of improvement. And knowing environmental effect can give us a deeper understanding to the behavior of cellulose molecules, which can definitely contribute to future develop of cellulose-based materials.

In this chapter, original gels have been made under various humidity and temperature. The resulted change in structure and mechanical performance have been checked. The cellulose molecules flexibility in original state plays an important role in the final morphology and mechanical performance of DCC samples.

3.2 Experimental

3.2.1 Materials

Cellulose source (Advantec filter paper, Toyo Roshi Kaisha Ltd., Japan), DMAc and lithium chloride (Tokyo Chemical Industry Co., Ltd, Japan), acetone (Kanto Chemical Co., Inc.,

Japan), and ethanol (Imazu Chemical Co., Ltd.) were used as received without further purification. All the aqueous solutions were prepared using ultrapure deionized water.

3.2.2 Gels preparation

Cellulose hydrogels were prepared from filter papers, as previously reported, with some minor difference.9 The cut filter paper sheets were sequentially washed with water and ethanol. The washed paper was then activated by immersion in DMAc for 12 h and then vacuum dried at 60 °C. To prepare the cellulose solution, 0.75 g activated cellulose was dissolved in 100 g of LiCl/DMAc (8 g: 92 g). The cellulose solution was cast into a glass mold with a thickness of 3 mm. The solution was left in air under ambient conditions (temperature, 20 °C; humidity, 20%). After 2 days, the solution became a weak gel due to the diffusion of water molecules from the air into the cellulose solution. The weak cellulose gel was then placed in pure water and equilibrated for 2 days, changing the water every 12 h, to obtain the cellulose hydrogel (thickness ~2 mm). The cellulose hydrogels were cut into small pieces 10 mm wide, and 40 mm long and ~2 mm thick, and then loaded into the clamping devices with an initial length between the clamps of 30 mm, as shown in Figure 1. Pre-strains of 0%, 20%, 50%, and 100%, were applied to different samples, keeping them dried at room temperature (humidity 10%–40%) while the length was fixed, to form DCC-W0%, DCC-W20%, DCC-W50%, and DCC-W100% hydrogels, respectively. After drying for 10 h, all dried samples were removed from the clamping devices and re-immersed in water to obtain the final DCC samples. For comparison, ND-W was also prepared through drying the cellulose hydrogel without any mechanical restriction at room temperature (humidity 10%-40%).

3.2.3 Tensile tests

Tensile tests of gels were conducted in air at room temperature (25 °C) using a commercial mechanical tester (Instron 5965). The tensile speed was 100 mm/min. The distance between the clamps was fixed at 30 mm. Three specimens were used to test each sample. A cyclic loading-unloading test with a strain of up to 20% was also carried out in a moist environment to prevent water evaporation. The waiting time between the cycles of each test was 30 min. Stress was defined as the force divided by the initial cross-sectional area of the sample. The fracture stress and fracture strain were defined as the nominal stress and strain at the fracture point, respectively. The Young's modulus E was defined as the value of the initial slope of the stress–strain curve.

3.2.4 SEM observation

The structures of the samples were characterized by SEM (JSM-6010LA, JEOL Ltd.). To prepare the sample for SEM observation, hydrated samples were freeze-dried using a freeze-drying device (Advantage XL-70, VirTis) and coated with gold using an ion-sputtering device (E-1010, Hitachi, Japan). Changes in the shapes and volumes of the samples were not observed after freeze-drying.

3.3 Results and discussion

Figure 2.1 shows the process of preparation of original cellulose hydrogel, in the step of formation of physical gel, or say DMAc/Cellulose gel, the environmental conditions show obvious effect to the property of original cellulose hydrogels.

3.3.1 Environmental effect on the structure and mechanical property of original cellulose gels

First, cellulose solutions were placed in different humidity, 80%, 45% and 20% respectively, temperature was kept under an constant level which is around 25 ℃. As shown in Figure 2.2, high humidity will accelerate the formation of DMAc/Cellulose gel and induce a deformed shape of original cellulose hydrogels. The higher the humidity is, the shape become more deformed. The reason for this phenomenon might be that cellulose molecules will absorb more water from the interface under high humidity environment, and driving by the hydrophobic backbone of cellulose molecules, drastic aggregation of molecules started from the interface. And we found that the volume of original cellulose hydrogel is related to the volume of DMAc/Cellulose gel. As shown in Figure 2.3a, to better control the volume, we keep the DMAc/Cellulose gel under stale environmental condition, 25 ℃, ~20% humidity, the volume will keep shrinking when keep the DMAc/Cellulose gel drying under air. And after drying for different days, we did solvent exchange, with water and ethanol respectively, however different the volume of DMAc/gels are, the volume of original hydrogels also show a decreased volume accordingly. Under the observation of SEM, as shown in Figure 2.3b, we confirmed longer evaporating time during DMAc/Cellulose gel drying process, the fibrous structure inside original hydrogel became denser. But the interesting thing is that, according to the tensile tests result, denser fibrous structure didn't constantly enhance the mechanical performance, the original cellulose hydrogel shows best fracture stress and fracture strain when evaporating time is 2 day, as shown in Figure 2.4. So far, the fibrous morphology and mechanical performance of original cellulose hydrogel is a result of

cellulose molecules aggregation. And this aggregation behavior can be controlled through humidity, and evaporating time of DMAc/Cellulose. Here we consider the 2 days evaporating time under 25 ℃, 20% humidity environment is the ideal condition, because the resulted original cellulose hydrogel is flat on the surface, and most stretchable, which is a favored property to pursue high strength by DCC method afterwards. In the following parts, if there is no mention, the environment for evaporation of solvent are all 25 ℃ and 20% humidity.

3.3.2 Environmental effect on the structure and mechanical property of DCC-Cellulose hydrogels

DCC method are tried under different conditions, with the purpose to control the drying speed. We set 3 three temperatures, 5℃, 25℃ and 60℃. So under each environment, the drying speed is slow, moderate and fast. Samples prepared under low and moderate temperature show no change in mechanical performance, while high temperature induced a little decline in fracture stress and fracture stain. Considering under ambient environment, temperature will always be controlled within 20~30 ℃, so the temperature effect on the mechanical performance of DCC samples are limited.

But we also checked how will fast evaporating speed affect the fibrous structure. Under temperature 60 ℃, as we can see in Figure 2.7, fibril bundles are not so separated compare with room temperature sample, to further confirm the temperature effect, we tried DCC method under 80℃ with vacuum environment, under which, water evaporate so fast that fibril just simply attached to each other before finely aggregated into fibril bundles.

3.4 Conclusions

By preparing original cellulose hydrogel under different humidity, we confirmed that 25℃ 20% humidity are the optimum conditions, because original cellulose hydrogel prepared under this environment show ideal shape, and stretchability. Then DCC method was applied to the original cellulose hydrogels under different temperature. High temperature will induce a fast crosslinking between fibrils, and resulted sample show a fibril bundles that not well separated. The process of aggregation of fibrils into fibril bundles need sufficient time space.

3.5 References

[1] M. T. I. Mredha, Y. Z. Guo, T. Nonoyama, T. Nakajima, T. Kurokawa, J. P. Gong, A Facile Method to Fabricate Anisotropic Hydrogels with Perfectly Aligned Hierarchical Fibrous Structures. Adv. Mater. 30 (9) (2018) 1704937. https://doi.org/10.1002/adma.201704937

[2] W. Zhang, S. Okubayashi, T. Bechtold, Fibrillation tendency of cellulosic fibers. Part 1: Effects of swelling. Cellulose. 12 (2005) 267–273. https://doi.org/10.1007/s10570-004-2786-z

3.6 Figures

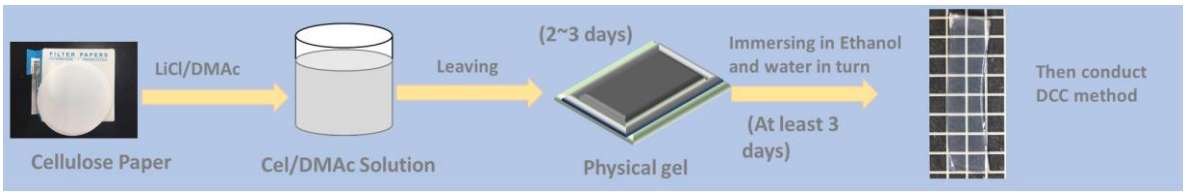

Figure 3.1 Process of preparation of Cellulose hydrogel.

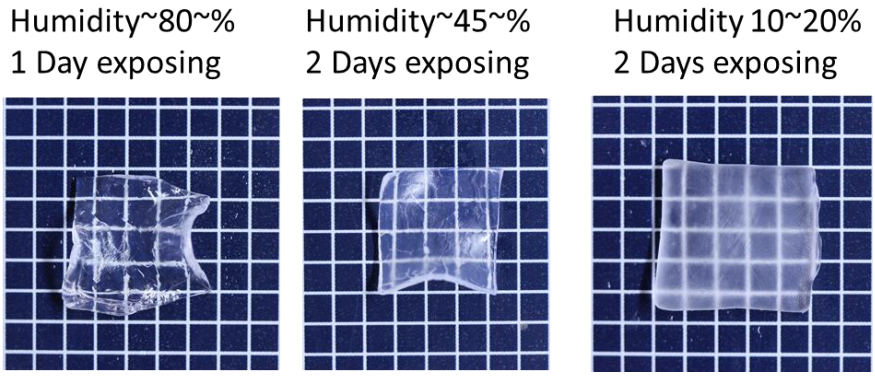

Figure 3.2 Cellulose hydrogels prepared by exposing DMAc/Cellulose gels under different humidity.

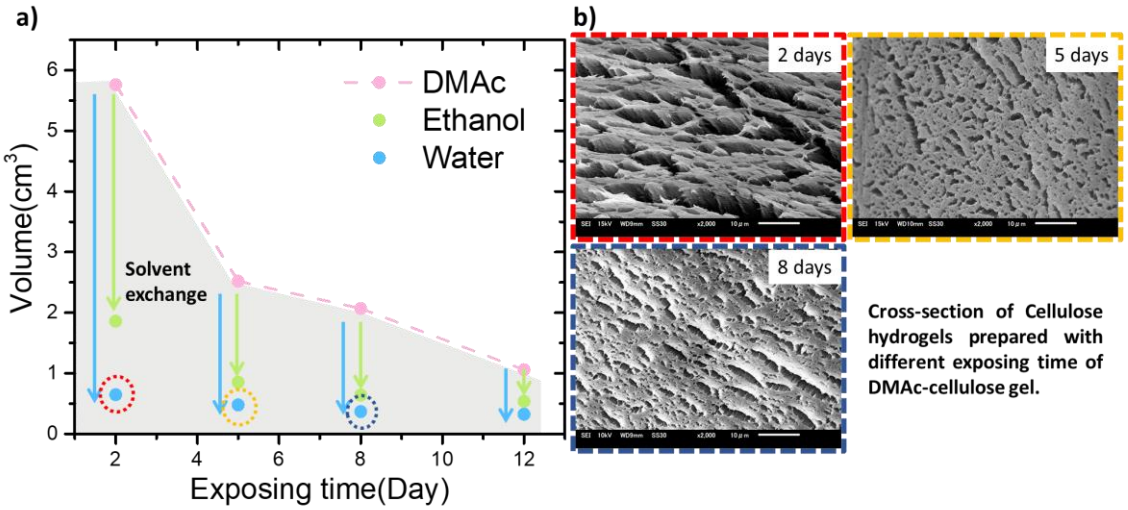

Figure 3.3 a) Volume change of DMAc-Cellulose gel after different exposing days. Green dots and blue dots showing the volume change of DMAc-Cellulose gels after solvent exchange with ethanol and water respectively. b) SEM observation on the cross-section of cellulose hydrogel prepared with different exposing time of DMAc-Cellulose gel.

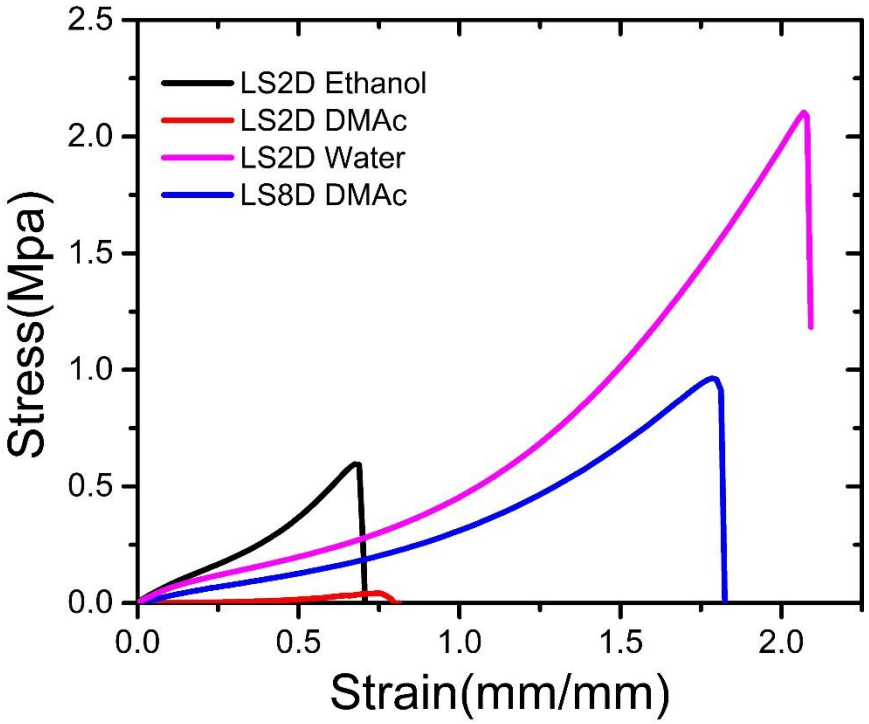

Figure 3.4 Tensile tests on cellulose gels with different conditions. *LS2D Ethanol means original DMAc gel was put under ambient condition(25 ℃, Hum ~20%) for 2 days and then do solvent exchange with ethanol. *LS2D DMAc means original DMAc gel was put under ambient condition (25 ℃, Hum ~20%) for 2days and then do tensile tests without solvent exchange.

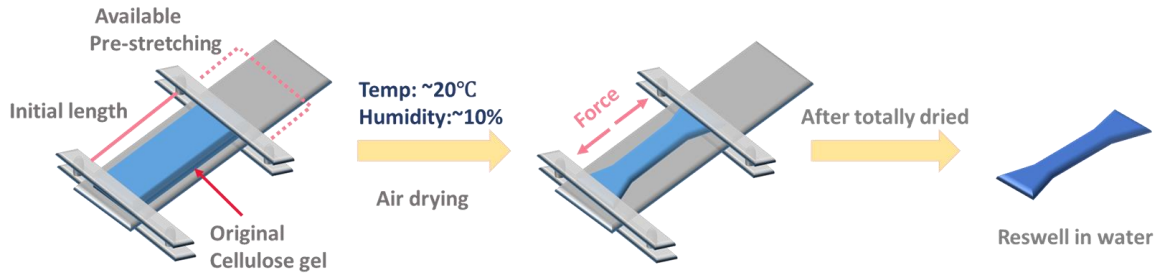

Figure 3.5 Schematic illustration of DCC method

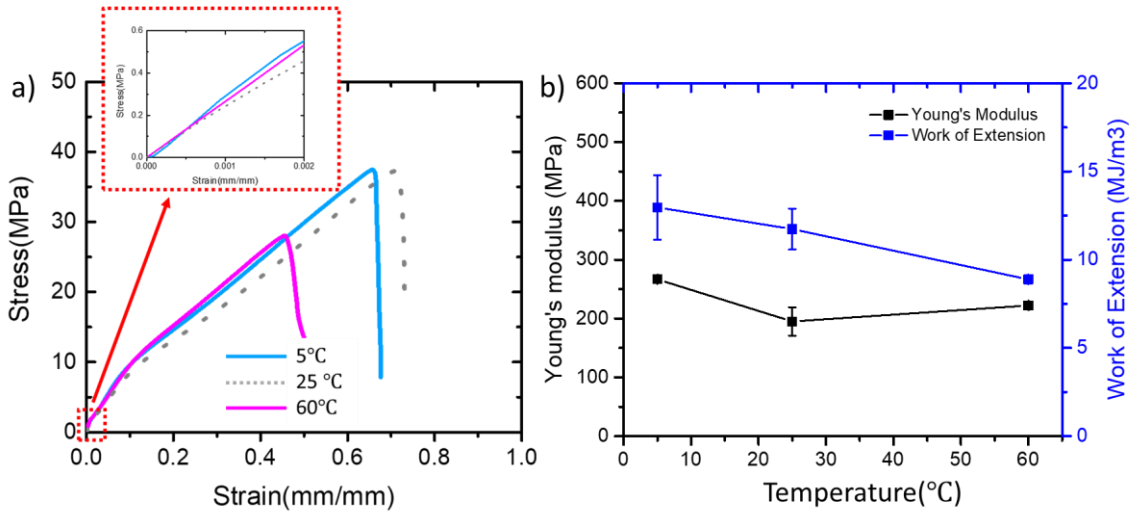

Figure 3.6 a) Tensile tests of DCC samples dried under different temperature. b) The change of mechanical performance of DCC samples with the temperature during drying process.

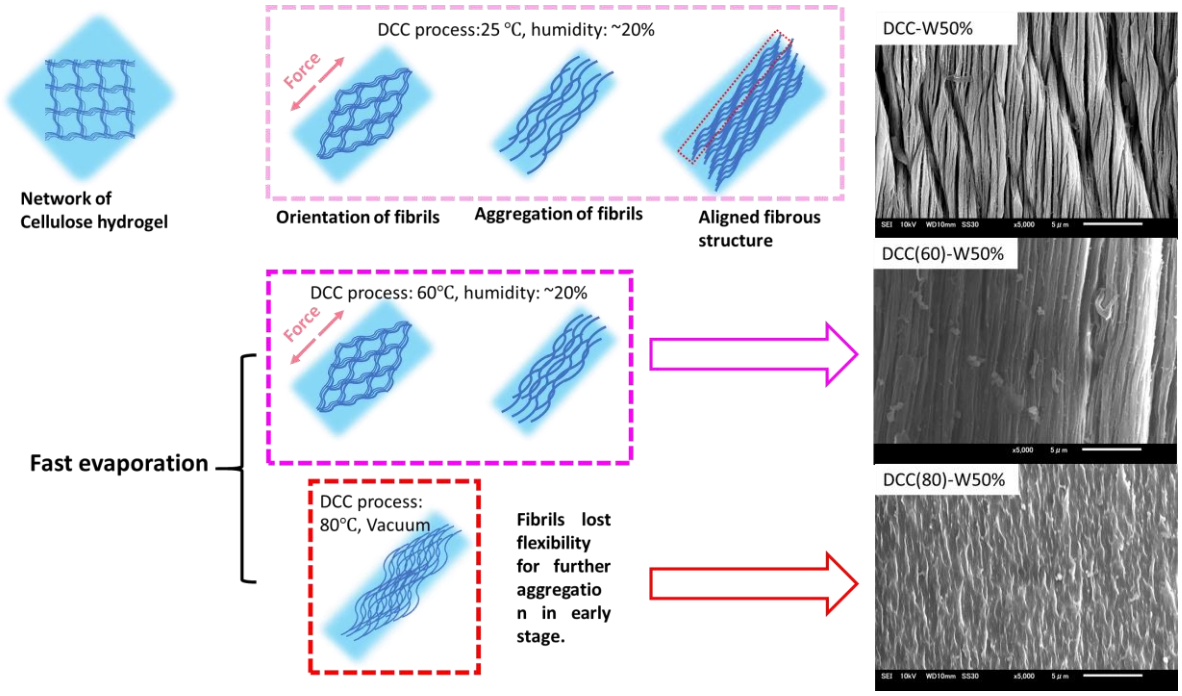

Figure 3.7 Schematic illustration of structure evolution during DCC method under different temperature.

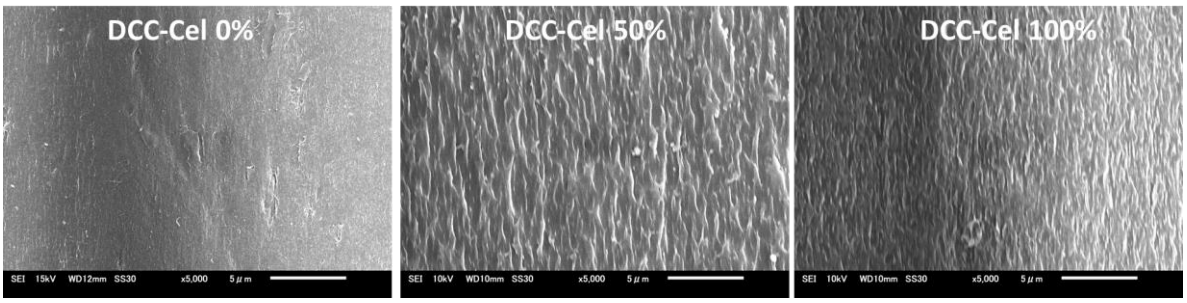

Figure 3.8 Morphology of DCC samples under 80°C, vacuum condition.

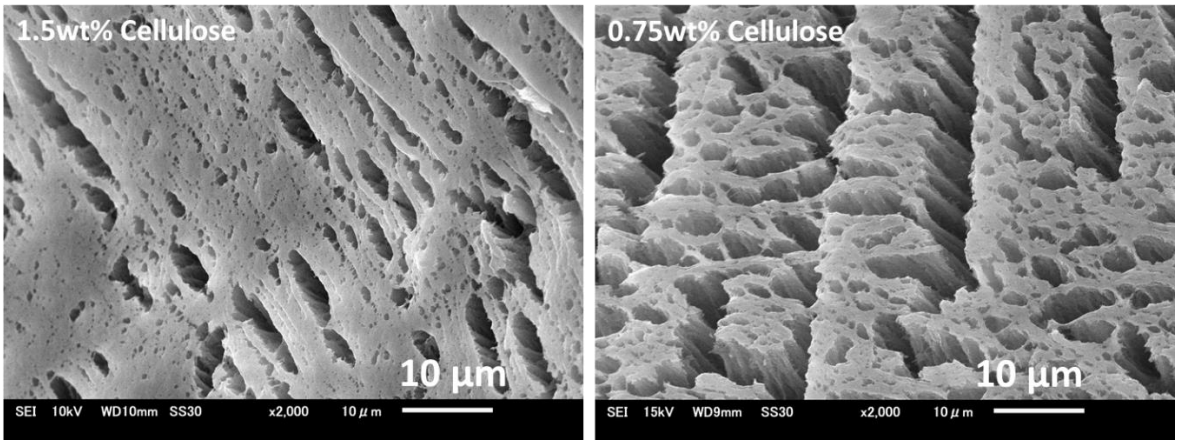

Figure 3.9 SEM observation on the cross-section of cellulose hydrogel with different cellulose content.

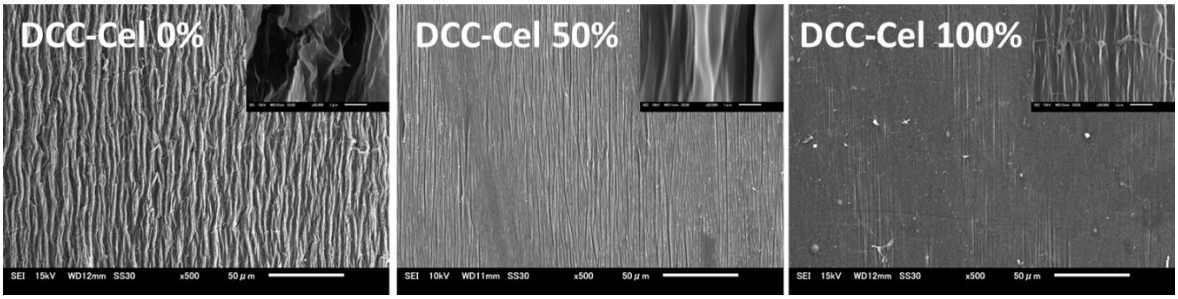

Figure 3.10 SEM observation on the surface of DCC-Cellulose hydrogels with 1.5 wt% cellulose.

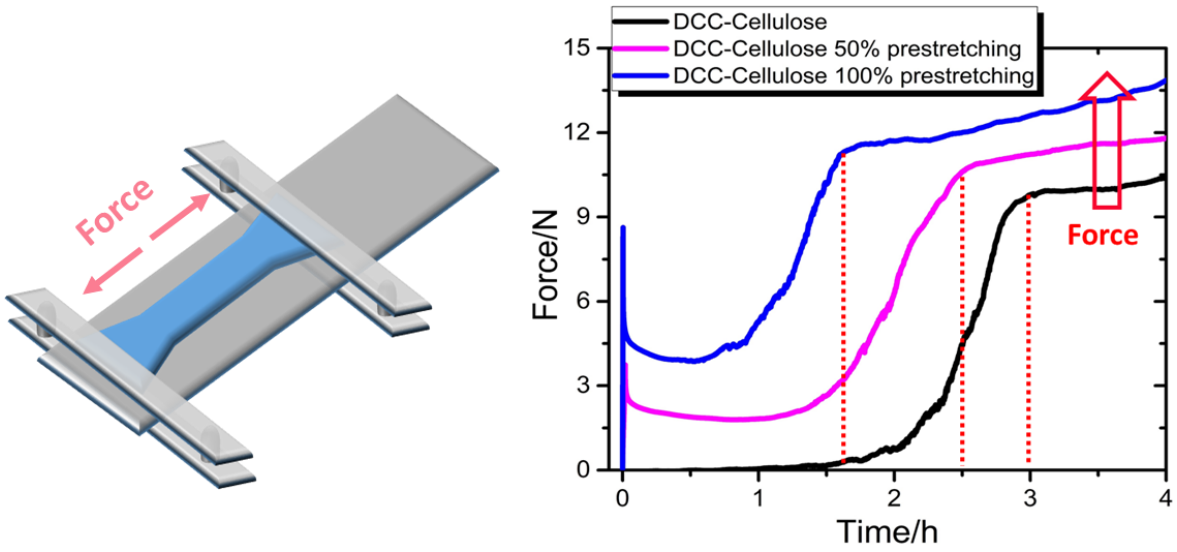

Figure 3.11 Force change during DCC method

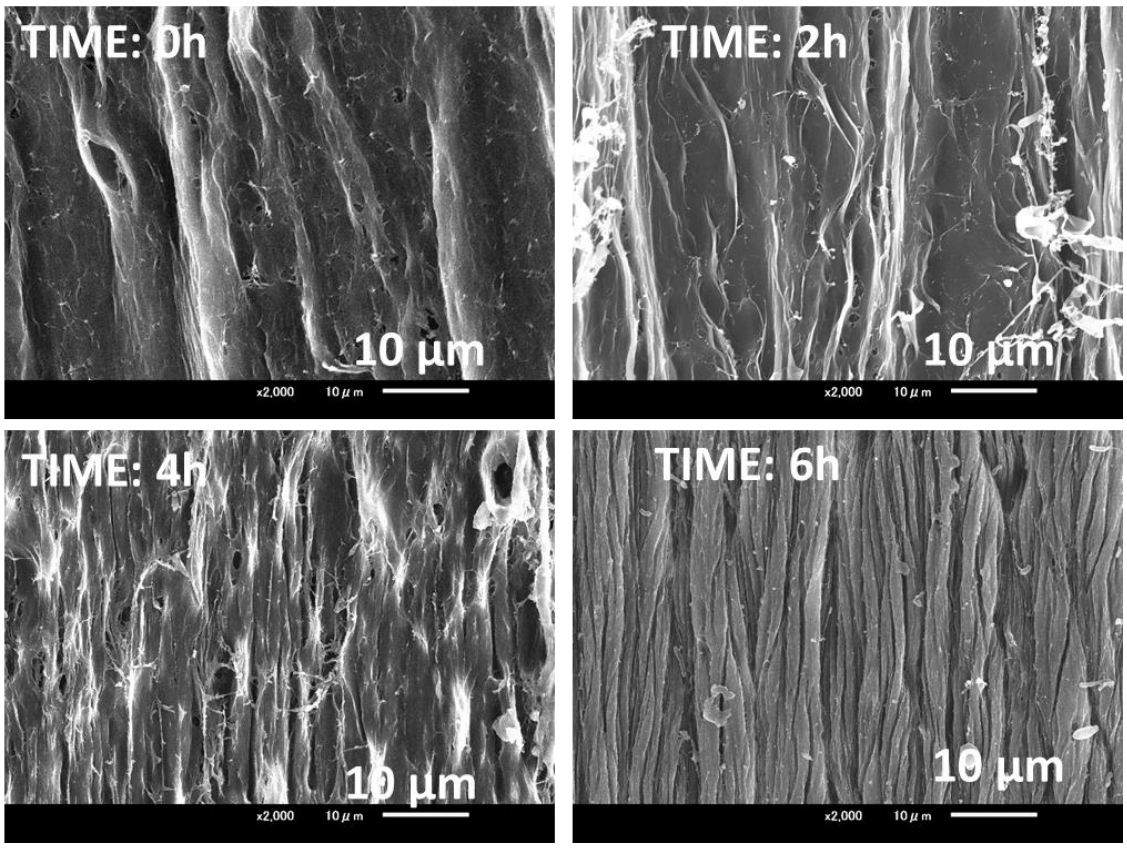

Figure 3.12 SEM observation on the morphology of DCC-Cel with different drying hours.

CHAPTER 4

Facile preparation of cellulose hydrogel with achilles tendon-like super strength through aligning hierarchical fibrous structure

4.1 Introduction

Polymer hydrogels are polymeric materials containing a large volume of water inside. This water-rich nature makes hydrogels similar to biological tissues, so that they are potentially suitable for use as biomaterials, including wearable devices, soft robotics, and alternative materials for various biological tissues.[1] However, the lack of sufficient strength and toughness restricts the application prospects of hydrogels. It is particularly challenging to fabricate hydrogels with excellent mechanical properties that could replace fibrous connective tissues such as ligaments and tendons. In recent years, different strategies, such as a double network strategy,[2,3] hybridization with nanomaterials,[4,5] and the use of biopolymers such as polysaccharides or proteins,[6,7] have been attempted to pursue the mechanical performance of fibrous connective tissues. However, hydrogels with strength at

the level of the Achilles tendon (fracture stress ~80 MPa, Young's modulus ~800 MPa)[8] have not yet been reported.

Fibrous connective tissues have a hierarchical structure in which biopolymers such as collagen form fibrous aggregates, and the fibers are further aligned unidirectionally. Inspired by this hierarchical structure, we have previously developed a facile method to prepare strong biopolymer hydrogels with highly aligned hierarchical fibrous structures. This method was called the drying under confined conditions (DCC) method.[9] In the DCC method, as shown in Figure 4.1, typical biopolymer hydrogels were uniaxially pre-stretched and dried with the length fixed. The drying process induces fibrillization of biopolymers, and length confinement leads to unidirectional orientation of the fibers. After reswelling in water, biopolymer gels with superior strength and a unidirectionally aligned fibrous structure, called DCC hydrogels, were obtained. With higher pre-stretching of the original biopolymer hydrogels, the fibrous structure of the DCC hydrogels became more aligned, and the strength along the stress direction also increased. In this previous study, we used a cellulose hydrogel as an original biopolymer gel, which was prepared from cellulose solution by dialysis with water as an anti-solvent and pre-stretched it to its stretching limit for the DCC method (pre-stretching ratio of 100%). An optimized DCC cellulose hydrogel reached outstanding fracture stress (~55 MPa) and modulus (~340 MPa) parallel to the pre-stretching direction.[9] Although the strength and stiffness of these reported DCC hydrogels are superior to those of other man-made hydrogels, the strength at the level of the Achilles tendon is still far from reaching.

To further improve the mechanical properties of DCC cellulose gels, we thought that the degree of orientation of the cellulose fibrous structure needs to be improved. To solve this issue, we investigated the internal structure of the original cellulose hydrogel, which was obtained by the regeneration method from the cellulose dissolved in a LiOH/N,N-dimethylacetamide (DMAc) mixture (Figure 4.2). Several papers have reported that the aggregation structure of regenerated cellulose depends on the anti-solvent used for regeneration.[10-12] If pure water is used as the anti-solvent, abundant cellulose fibrils form inside the cellulose hydrogels before the drying process (Figure 4.3). Such pre-ordering of the cellulose fibrils in the original gels may impede the formation of well-oriented cellulose fibrils during the DCC method. On the other hand, if ethanol is used as the anti-solvent, cellulose forms a relatively loose and disordered structure.[13] If such relatively loose cellulose is used as the starting material for the DCC method, the strength can be further improved by the DCC method.

In this study, we chose to conduct the DCC method on cellulose alcogels (gels with ethanol as solvent), because cellulose molecules are less aggregated in ethanol solvent, which gives cellulose alcogels a larger swelling ratio,[13] and hence more stretched cellulose molecules. Then, using the DCC method with 50% pre-stretching, we successfully prepared a super strong DCC cellulose hydrogel (DCC-E50%), with a fracture stress > 80 MPa, which already reaches the level of a human Achilles tendon, and a Young's modulus > 500 MPa. Although strength enhancement of most materials only occurs at the expense of toughness,[14] we found that, there was no compromise in toughness despite significant improvements in strength. Through scanning electron microscopy (SEM) and small-angle X-ray scattering

(SAXS), and wide-angle X-ray diffraction (WAXD) characterizations, we confirmed that the fibrous structure of the DCC-E samples showed a rather different arrangement, which could play a central role in the improvement of both strength and toughness.

4.2 Experimental

4.2.1 Materials.

Cellulose source (Advantec filter paper, Toyo Roshi Kaisha Ltd., Japan), DMAc and lithium chloride (Tokyo Chemical Industry Co., Ltd, Japan), acetone (Kanto Chemical Co., Inc., Japan), and ethanol (Imazu Chemical Co., Ltd.) were used as received without further purification. All the aqueous solutions were prepared using ultrapure deionized water.

4.2.2 Preparation of cellulose hydrogel.

Cellulose hydrogels were prepared from filter papers, as previously reported, with some minor difference.[9] The cut filter paper sheets were sequentially washed with water and ethanol. The washed paper was then activated by immersion in DMAc for 12 h and then vacuum dried at 60 °C. To prepare the cellulose solution, 0.75 g activated cellulose was dissolved in 100 g of LiCl/DMAc (8 g: 92 g). The cellulose solution was cast into a glass mold with a thickness of 3 mm. The solution was left in air under ambient conditions (temperature, 20 °C; humidity, 20%). After 2 days, the solution became a weak gel due to the diffusion of water molecules from the air into the cellulose solution. The weak cellulose

gel was then placed in pure water and equilibrated for 2 days, changing the water every 12 h, to obtain the cellulose hydrogel (thickness ~2 mm). The cellulose hydrogels were cut into small pieces 10 mm wide, and 40 mm long and ~2 mm thick, and then loaded into the clamping devices with an initial length between the clamps of 30 mm, as shown in Figure 4.1. Pre-strains of 0%, 20%, 50%, and 100%, were applied to different samples, keeping them dried at room temperature (humidity 10%–40%) while the length was fixed, to form DCC-W0%, DCC-W20%, DCC-W50%, and DCC-W100% hydrogels, respectively. After drying for 10 h, all dried samples were removed from the clamping devices and re-immersed in water to obtain the final DCC samples. For comparison, ND-W was also prepared through drying the cellulose hydrogel without any mechanical restriction at room temperature (humidity 10%-40%).

4.2.3 Preparation of cellulose alcogel.

Cellulose alcogels were prepared using the same procedure as the cellulose hydrogel until the formation of the weak gel. The weak cellulose gel was solvated in ethanol instead of water for 2 days, changing the ethanol every 12 h, to obtain ethanol cellulose gels (thickness ~3 mm). Samples were cut ~3 mm thick, 10 mm wide, and loaded into the clamping device with 30 mm length between the two clamped ends. Pre-strains of 0%, 20%, and 50%, were applied to different samples, keeping them dried at room temperature (humidity 10%–40%) while the length was fixed, to form DCC-E0%, DCC-E20%, and DCC-E50% hydrogels, respectively.

4.2.4 Material Characterization.

Swelling Ratio. The 1D swelling ratio in different directions is defined as i/i0, where i is the thickness, width, or length of the swollen sample, and i0 is that of the corresponding dried sample.

Water content: The water content (H0) of the gels was calculated using the equation H0 = (Hs - Hd)/Hs, where Hs is the weight of the gel in the fully swollen state and Hd is the weight after freezing-drying.

Light transmittance test. The light transmittance of cellulose hydrogels and alcogels was measured using a Shimadzu UV spectrophotometer (UV-1800) at wavelengths from 200 to 800 nm. For the measurement, the hydrogel and alcogel samples were placed in a quartz cuvette filled with water and ethanol, respectively.

Mechanical properties. Tensile tests of gels were conducted in air at room temperature (25 °C) using a commercial mechanical tester (Instron 5965). The tensile speed was 100 mm/min. The distance between the clamps was fixed at 30 mm. Three specimens were used to test each sample. A cyclic loading-unloading test with a strain of up to 20% was also carried out in a moist environment to prevent water evaporation. The waiting time between the cycles of each test was 30 min. Stress was defined as the force divided by the initial cross-sectional area of the sample. The fracture stress and fracture strain were defined as the nominal stress and strain at the fracture point, respectively. The Young's modulus E was defined as the value of the initial slope of the stress–strain curve.

SEM observation. The structures of the samples were characterized by SEM (JSM-6010LA, JEOL Ltd.). To prepare the sample for SEM observation, hydrated samples were freeze-dried using a freeze-drying device (Advantage XL-70, VirTis) and coated with gold using an ion-sputtering device (E-1010, Hitachi, Japan). Changes in the shapes and volumes of the samples were not observed after freeze-drying.

X-ray scattering characterization. The cellulose gels were evaluated using SAXS and WAXD. Both SAXS and WAXD measurements were performed at beamline BL05XU at SPring-8 (Hyogo, Japan). The X-ray wavelength was 1 Å (12.4 keV in energy). In the SAXS measurements, the distance between the sample and detector was 3.8 m. The irradiation time was 5 s for each sample to obtain a 2D scattering image. In the WAXD measurement, the distance between the sample and the detector was 0.066 m. The irradiation time was 3 s for each sample to obtain a 2D scattering image. In both measurements, the stretching direction of the sample was vertical.

4.3 Results and Discussion

4.3.1 Cellulose hydrogel and alcogel before DCC method

We first prepared both the cellulose hydrogel and the cellulose alcogel (Figure 4.2). Figure 4.4a shows digital photographs of the hydrogel and alcogel, which contain the same amount of cellulose. The cellulose alcogel had three times the volume of the cellulose hydrogel. Furthermore, by using ultraviolet–visible (UV-Vis) spectroscopy on both the cellulose hydrogel and alcogel, as shown in Figure 4.4c, we confirmed that the cellulose alcogel, even

with a higher thickness, has a higher transmittance over a wide range of wavelengths. These data suggest a less aggregated structure of cellulose in the alcogel than in the hydrogel. Figure 4b shows the stress-strain curves of the cellulose hydrogel and alcogel. These stress-strain curves are typical S-shaped curves found in rubbery elastic materials, suggesting that the stress-strain behavior mainly reflects the elasticity of the cellulose network strands either single chain level or fibrils level.[15] The cellulose alcogel fractured at a lower strain than the cellulose hydrogel, however it also exhibited a significantly higher Young's modulus (0.8 MPa) than the cellulose hydrogel (0.43 MPa). There are two possible explanations for the brittleness and stiffness of the cellulose alcogel. One is the increase in cross-linking density, in which shorter and denser network strands lead to stiffness and brittleness.[16] The other is the straightening of strands, in which highly pre-stretched strands lead to brittleness and stiffness.[17] Considering the observed structure of the hydrogel and alcogel, the alcogel has a lower cellulose density and a less aggregated structure than the hydrogel; therefore, it is unlikely that the cross-linking density of the cellulose in the alcogel is significantly higher than that in the hydrogel. Thus, we conclude that the cellulose network strands in the stiff alcogel are sparse and straight, while those in the soft hydrogel are dense but more deformable, as illustrated in Figure 4d.

4.3.2 Swelling ratio and water content after DCC method

Subsequently, we applied the DCC method to cellulose alcogels and hydrogels. In particular, the swollen gels were uniaxially stretched to the desired pre-strain and dried while maintaining their length. The oriented fibrous structure of cellulose was formed inside the materials during the drying process. The dried gels were then re-immersed in pure water until

swelling equilibrium was reached to obtain the DCC hydrogels. Alcogel-based DCC hydrogels are referred to as DCC-E gels and hydrogel-based DCC hydrogels as DCC-W gels. Under the same pre-strain for the DCC method, fibrils formed inside DCC-E gel would be more oriented than DCC-W gel, because the network strands in the alcogel are initially straight, and there is more space for better aggregation during drying.

Then, the one-dimensional (1D) swelling ratios in three different directions (length, width, and thickness) of the DCC hydrogels were investigated, as shown in Figure 4.5a. All DCC-E and DCC-W gels showed anisotropic swelling behaviour after immersion in water. The reswollen DCC samples show no obvious swelling in length direction, while there was significant swelling in the other two directions; for example, Figure 4.5b shows photos comparing DCC-W50% before and after reswelling. The one-directional swelling ratios in width and thickness depend slightly on the pre-strain and original solvent of the DCC hydrogels. The water content of all DCC hydrogels dropped from above 90% (original gels) to approximately 55%, as shown in Figure 4.5c. The anisotropic swelling behavior and decreased water content indicate abundant fibrillization along the tensile stress direction.[18, 19] Fibrillization of cellulose by drying works as cross-links to suppress the water content of the DCC hydrogels, and the formation of stiff and highly aligned fibrils deters swelling in the length direction.

4.3.3 Mechanical properties of DCC hydrogels

Although all the DCC samples showed similar water content (~55%) regardless of their original solvent and pre-strain, their mechanical properties varied significantly, as shown in

Figure 4.6a and Table 1. When comparing the uniaxial stress-strain curves of the DCC-E and DCC-W samples, we found that the DCC-E samples showed a higher fracture stress and Young's modulus (Figure 4.7) than the corresponding DCC-W samples with the same pre-strain. In particular, we would like to emphasize a super-high fracture stress (above 80 MPa) and Young's modulus (above 500 MPa) for the DCC-E50% samples. The fracture stress of a hydrogel at this level is comparable to that of the Achilles tendon of a human adult (Table 1), which has rarely been reported in hydrogel works. To demonstrate such extreme strength, we lifted a 5 kg weight and moved it up and down with a DCC-E50% sample 45 mm long, ~0.5 mm thick, and ~2 mm wide, as shown in the Supporting Movie S1 and Figure 4.6b.

The DCC-E gels are not just an optimization of the conventional DCC(-W) system but represent an improved class of materials. To clarify the improved performance of the DCC-E gels compared with the DCC-W gels, we plotted the fracture strain against the fracture stress for all DCC samples in Figure 4.6c. For each of the DCC-E and DCC-W samples with different pre-strains, trade-off trends were observed between the fracture stress and fracture strain. On the other hand, the trend for the DCC-E samples shifted to the upper right compared to the DCC-W samples in the graph. These results show that the DCC method works more effectively on cellulose alcogel by providing DCC-E samples with increased fracture stress but a slower decrease in the fracture strain than the corresponding DCC-W samples.

The shift of the fracture stress-strain curve to the upper right indicates an increase in the energy required to break the samples (toughness). To characterize toughness, we calculated

the work of extension (W), defined as the area under the stress-strain curves until sample fracture. We plotted the work of extension (W) against the Young's modulus (E) for all DCC samples, as shown in Figure 4.6d. The curve for the DCC-W samples shows a typical relationship between Young's modulus and toughness of materials, which is the modulus increase at the expense of toughness. For the DCC-E samples, however, the modulus increased by increasing the pre-strain without sacrificing toughness. This means that the DCC-E gels can have a tunable modulus while maintaining high toughness. This modulus tunability makes the DCC-E gels suitable for use as alternative materials for various fibrous tissues needing a wide stiffness range, such as tendons and ligaments.

4.3.4 Energy dissipation behavior of DCC hydrogels

To understand how DCC-E samples can maintain a high modulus, strength, and toughness, we performed cyclic tensile tests to study the energy dissipation behavior of all the DCC samples, as shown in Figure 4.8a. All the DCC samples showed significant mechanical hysteresis in the first cycle with a maximum strain of 0.2, suggesting a large energy dissipation during stretching. After the first cycle, the samples were left in a moist environment for 30 min. In the second cycle, a smaller mechanical hysteresis is observed. These data indicate that some of the dissipated energy in the first cycle is recoverable under ambient conditions, while the rest is dissipated quasi-permanently. The quasi-permanent energy dissipation indicates an irreversible structural transition of the DCC samples during stretching. By further comparison of the hysteresis between DCC-E and DCC-W samples, as shown in Figure 4.8b, we found that DCC-E samples dissipate more energy than the

corresponding DCC-W samples with the same pre-strain, and the DCC-E samples show a smaller recovery ratio than the DCC-W samples.

Figure 4.8c depicts the residual strain of the DCC samples immediately after the first cycle and after 30 min of waiting. Each sample showed a significantly high residual strain, which corresponded to the energy dissipation during the cyclic test. The residual strain tended to be higher as the pre-strain increased, and the DCC-E gels showed a higher residual strain than the DCC-W gels with the same pre-strain. This tendency is similar to that of the energy recovery ratio. These data suggest a more efficient energy dissipation mechanism of the DCC-E samples upon deformation accompanying the structural transition and that the high toughness of the DCC-E samples originates from their efficient irreversible energy dissipation mechanism.

4.3.5 Structure characterization

Since all the prepared hydrogels are pure cellulose systems, the mechanical properties and energy dissipation mechanisms of the gels are highly dependent on the properties of cellulose fibrils and the morphology of the fibrils. To understand the structural origins of the enhancement of both the strength and toughness of the DCC-E samples, we used several techniques to characterize the fibril structure from the molecular level to the micrometer level for all the DCC samples.

It has been revealed that hierarchical structures exist extensively in biological tissues, playing an important role in toughening by dissipating energy to avoid devastating fractures.[20] Therefore, we observed freeze-dried DCC samples by SEM to observe their

hierarchical fibrous structures. Figures 4.9a to 4.9e show pictures of the DCC samples observed by SEM at different magnifications. In all cases, the aligned cellulose fibrils formed hierarchical bundles in the DCC samples, as previously reported.[9] For DCC-W samples, the fibrils form twisted bundles at various scales, such as at the μm (i, ii) and sub-μm (iii) levels, and the morphology of the twisted bundles is controlled by varying the pre-strain during the DCC process. As shown in Figures 4.9a-i and 4.9a-ii, DCC-W0% shows thick fibril bundles with widths of approximately 7–10 μm, while the fibrils are not well oriented. With higher pre-strain, the fibril bundles of DCC-W50% and DCC-W100% became thinner. The highest magnification images confirm that with higher pre-strain, fibrils are more oriented and aggregated more closely with each other. In the DCC-E samples, unlike in the DCC-W samples, the fibrils do not form twisted bundles at any level. Bundles were confirmed with more straight fibrils stacked in parallel. Further comparing Figure 4.9e-iii with Figure 4.9d-iii, with higher pre-strain, fibrils also became straighter and more tightly packed.

We also measured the diameter of the fibrils shown in Figures 4.9a-iii to 4.9e-iii to clarify how the diameter of unit fibrils changed under different environments. Here, the unit fibrils are the thinnest fibrils that can be detected in the SEM images. As shown in Figure S4, in all DCC samples, the diameter varied from approximately 100 nm to 200 nm.

SAXS measurements were performed on the DCC samples to analyze their nanoscale structure. The samples were aligned along the vertical direction, as shown in Figure 4.10 Figures 4.11a to 4.11e show the 2D scattering patterns of the DCC samples. Two scattering

spots along the vertical direction were observed in all samples. According to previous reports, these spots indicate a periodic lamellar arrangement of crystalline and amorphous cellulose regions along the fiber length direction.[21] Similar to most of the regenerated cellulose materials, the scattering from the lamellar structure was partially covered by the beam stop,[21, 22] which means that the structure length of the lamellar structure is larger than 115 nm (calculated from the 1D profile in the vertical direction in Figure S6a), which is consistent with the SEM observation. In addition, sharp equatorial streaks in the horizontal direction were observed. The streaks indicate the nanometer-scale highly anisotropic structure in the DCC samples aligned in the stress direction, which should correspond to the fibrous structure of cellulose or needle-shaped voids between the cellulose fibrils. With a higher pre-strain for the DCC method, sharper and longer equatorial streaks for the DCC samples were observed. In addition, the DCC-E samples show longer streaks than the corresponding DCC-W samples with the same pre-strain. This means that an increase in the pre-strain and use of ethanol as the original solvent led to a higher alignment of cellulose fibrils in the DCC samples.

WAXD measurements were performed on the DCC samples to analyze their molecular-scale structures. The DCC stretching of the samples was in the vertical direction, as shown in Figure 4.12. The 2D images of the WAXD for the DCC samples are shown in Figures 4.14a to 4.14f. For the cellulose hydrogel without DCC, only an amorphous scattering halo was observed, suggesting that the gel from regenerated cellulose was isotropic and had negligible crystalline domains. After applying the DCC method, two obvious changes were observed in the scattering profiles. First, instead of the amorphous scattering halo, two bright spots appeared in the horizontal direction, corresponding to the increased alignment of the non-

crystalline region. Second, crystalline signals appeared in the scattering profiles of all DCC samples. The peaks can be assigned to cellulose II,[23, 24] as shown in the 1D profiles (Figures 4.15 and 4.15). From the 2D patterns of the WAXD results, for both DCC-W and DCC-E samples, the orientation of the crystalline region seems to be stronger with an increase in pre-strain. To quantify the orientation degree, we calculated the FWHM value of the scattering plane (110), which is the strongest crystalline signal in all samples (Figure 4.14g). A smaller FWHM value indicates a higher degree of alignment of the crystals, and vice versa.[25] As shown in Figure 4.14h, the FWHM of the scattering plane (110) of both the DCC-W and DCC-E samples decreases with the pre-strain, suggesting that a larger pre-strain induces a higher degree of alignment of the cellulose crystals. Moreover, comparing the samples with the same pre-strain, the DCC-E gels showed a smaller FWHM than the DCC-W gels, implying better orientation of the cellulose crystals in the DCC-E gels.

WAXD and SAXS measurements clarified the enhanced orientation of cellulose in the DCC-E samples from molecular to fibril scales.

With the above structural information, we believe that there are two important structural changes that could account for the improvement in both strength and toughness of the DCC-E samples compared to the DCC-W samples. First, when comparing the DCC samples with the same pre-strain, the fibrils in the DCC-E gels have a stronger orientation than those in the DCC-W gels. Second, the fibrils inside the DCC-E gel were straight and in close contact, while the fibrils inside the DCC-W gel were twisted and loosely contacted. As already discussed, the difference in the fibrous structure of the DCC hydrogels depending on the

original solvent is due to the structural difference between the original cellulose alcogel and hydrogel. The cellulose alcogel contains straight and sparse cellulose molecules. Thus, during the DCC process, the more stretched molecules have a better chance to closely stack together along the stress direction to form straight fibrils and bundles when they have more free space available. On the other hand, in the cellulose hydrogel molecules have already twisted and aggregated to form fibrils;[26, 27] dense physical cross-linking suppresses the monodirectional aggregation of fibrils in the DCC process, leading to twisted and less dense fibril bundles in the DCC-W samples.

Here, we discuss the origin of the enhanced mechanical properties of DCC-E gels with these structural differences. For modulus enhancement, the degree of orientation of the fibrils should be a key factor. DCC-W gels consist of twisted fibrils, whereas DCC-E gels are composed of straight fibrils. Such straight fibrils generate larger stress than the twisted fibrils when stretched along the length direction, contributing to the enhanced Young's modulus of the DCC-E gels. For toughness and strength enhancement, the energy dissipation due to friction between the fibrils might be a key factor. Considering the fibrous structure of cellulose in the DCC samples, a large residual strain with irreversible energy dissipation of the DCC samples should correspond to the sliding of fibrils with large frictional energy dissipation. [28, 29] Cellulose in the DCC samples forms multiscale bundles via hydrogen bonding between the hydroxyl groups. In the DCC-E samples with tightly packed cellulose bundles, more hydrogen bonding would be formed between the molecules or bundles; hence, more energy would be stored inside in comparison with the DCC-W samples with twisted fibrils. During uniaxial stretching, energy is mainly dissipated by breaking the hydrogen

bonding between fibrils through friction, because fibrils are too strong to break at first. Therefore, DCC-E samples with straighter fibrils and thicker fibril bundles would dissipate more energy compared with the corresponding DCC-W samples. Such a large energy dissipation of the DCC-E gels also contributes to their high strength. Tensile fracture is caused by the propagation of a crack in a material from an initial defect. To prevent tensile fracture and realize high strength, it is important to prevent stress concentration at the defect. The energy dissipation mechanism in materials works to prevent such stress concentration. Because the DCC-E gels have a more effective energy dissipation mechanism than the DCC-W gels, the stress concentration is effectively prevented in the former system, leading to higher fracture strength.

4.4 Conclusion

We successfully created DCC-E hydrogels, characterized by a Young's modulus and fracture stress close to the level of the Achilles tendon in the human body. The key is to use ethanol as the anti-solvent for the preparation of the original cellulose gels (alcogels) for the DCC process, which leads to sparser and straighter network strands of the cellulose alcogels compared to the cellulose hydrogels. The main reason for the significant improvement in mechanical properties is attributed to be the higher degree of cellulose orientation observed in the DCC-E gels from the molecular scale to the submicron fibril scale. We confirmed this observation by hierarchical structural analyses using SEM, SAXS, and WAXD. Finally, this study provides a simple strategy to improve and modulate the mechanical performance of

biopolymer materials by controlling the fibril arrangement, which could expand the application field of biopolymers to tissue engineering and soft electronics.[30, 31]

4.5 References

[1] Y. S. Zhang, Ali. Khademhosseini, 2017. Advances in Engineering Hydrogels. Science. 356, eaaf3627. https://doi.org/10.1126/science.aaf3627

[2] J. P. Gong, Y. Katsuyama, T. Kurokawa, Y. Osada, Double-Network Hydrogels with Extremely High Mechanical Strength. Adv. Mater. 15 (14) (2003) 1155-1158. https://doi.org/10.1002/adma.200304907

[3] F. Yang, J. Zhao, W. J. Koshut, J. Watt, J. C. Riboh, K. Gall, B. J. Wiley, A Synthetic Hydrogel Composite with the Mechanical Behavior and Durability of Cartilage. Adv. Funct. Mater. 30(36), (2020) 2003451. https://doi.org/10.1002/adfm.202003451

[4] X. F. Wang, J. Fang, W. W. Zhu, C. X. Zhong, D. D. Ye, M. Y. Zhu, X. Lu, Y. S. Zhao, F. Z. Ren, Bioinspired Highly Anisotropic, Ultrastrong and Stiff, and Osteoconductive Mineralized Wood Hydrogel Composites for Bone Repair. Adv. Funct. Mater. 31(20), (2021) 2010068. https://doi.org/10.1002/adfm.202010068

[5] N. Annabi, S. R. Shin, A. Tamayol, M. Miscuglio, M. A. Bakooshli, A. Assmann, P. Mostafalu, J. Y. Sun, S. Mithieux, L. Cheung, X. S. Tang, A. S. Weiss, A. Khademhosseini, Highly Elastic and Conductive Human-Based Protein Hybrid Hydrogels. Adv. Mater. 28 (1) (2016) 40-49. https://doi.org/10.1002/adma.201503255

[6] C. Wu, J. Huang, B. Chu, J. Deng, Z. Zhang, S. Tang, X. Wang, Z. Wang, Y. Wang, Dynamic and Hierarchically Structured Networks with Tissue-like Mechanical Behavior. ACS Nano. 13 (9) (2019) 10727-10736. https://doi.org/10.1021/acsnano.9b05436

[7] Y. N. Zhang, R. K. Avery, Q. Vallmajo-Martin, A. Assmann, A. Vegh,; A. Memic, B. D. Olsen, N. Annabi, A. Khademhosseini, A Highly Elastic and Rapidly Crosslinkable Elastin-Like Polypeptide-Based Hydrogel for Biomedical Applications. Adv. Funct. Mater. 25 (30) (2015) 4814-4826. https://doi.org/10.1002/adfm.201501489

[8] T. A. L. Wren, S. A. Yerby, G. S. Beaupré, D. R. Carter, Mechanical Property of The Human Achilles Tendon. Clin Biomech. 16 (3) (2001) 245-251 https://doi.org/10.1016/S0268-0033(00)00089-9

[9] M. T. I. Mredha, Y. Z. Guo, T. Nonoyama, T. Nakajima, T. Kurokawa, J. P. Gong, A Facile Method to Fabricate Anisotropic Hydrogels with Perfectly Aligned Hierarchical Fibrous Structures. Adv. Mater. 30 (9) (2018) 1704937. https://doi.org/10.1002/adma.201704937

[10] X. Tan, L. Chen, X. Li, F. Xie, Effect of Anti-solvents on The Characteristics of Regenerated Cellulose from 1-ethyl-3-methylimidazolium Acetate Ionic Liquid. Int. J. Biol. Macromol. 124 (1) (2019) 314-320. https://doi.org/10.1016/j.ijbiomac.2018.11.138

[11] Z. Fan, J. Chen, W. Guo, F. Ma, S. Sun, Q. Zhou, Anti-solvents tuning cellulose nanoparticles through two competitive regeneration routes. Cellulose. 25 (2018) 4513–4523. https://doi.org/10.1007/s10570-018-1897-x

[12] K. M. Gupta, Z. Hu, J. Jiang, Cellulose regeneration from a cellulose/ionic liquid mixture: the role of anti-solvents. RSC Adv. 3 (2013) 12794-12801. https://doi.org/10.1039/C3RA40807H

[13] Z. Wang, S. Liu, Y. Matsumoto, S. Kuga, Cellulose gel and aerogel from LiCl/DMSO solution. Cellulose. 19 (2012) 393–399. https://doi.org/10.1007/s10570-012-9651-2

[14] R. O. Ritchie, The Conflicts Between Strength and Toughness. Nat. Mater. 10 (2011) 817-822. https://doi.org/10.1038/nmat3115

[15] J. E. Ritchie, B. Erman, C. M. Roland, The Science and Technology of Rubber, 4th ed.; Elsevier: Amsterdam, 2013.

[16] K. Y. Lee, J. A. Rowley, P. Eiselt, E. M. Moy, K. H. Bouhadir, D. J. Mooney, Controlling Mechanical and Swelling Properties of Alginate Hydrogels Independently by Cross-Linker Type and Cross-Linking Density. Macromolecules. 33 (11) (2000) 4291-4294. https://doi.org/10.1021/ma9921347

[17] H. Itagaki, T. Kurokawa, H. Furukawa, T. Nakajima, Y. Katsumoto, J. P. Gong, Water-Induced Brittle-Ductile Transition of Double Network Hydrogels. Macromolecules. 43 (22) (2010) 9495-9500. https://doi.org/10.1021/ma101413j

[18] J. M. B. F. Diniz, M. H. Gil,; J. A. A. M. Castro, Hornification—its origin and interpretation in wood pulps. Wood Sci. Technol. 37 (2004) 489-494. https://doi.org/10.1007/s00226-003-0216-2

[19] W. Zhang, S. Okubayashi, T. Bechtold, Fibrillation tendency of cellulosic fibers. Part 1: Effects of swelling. Cellulose. 12 (2005) 267–273. https://doi.org/10.1007/s10570-004-2786-z

[20] U. G. Wegst, H. Bai, E. Saiz, A. P. Tomsia, R. O. Ritchie,Bioinspired Structural Materials. Nat. Mater. 14 (2015) 23-36. https://doi.org/10.1038/nmat4089

[21] J. Cai, L. Zhang, J. Zhou, H. Qi, H. Chen, T. Kondo, X. Chen, B. Chu, Multifilament Fibers Based on Dissolution of Cellulose in NaOH/Urea Aqueous Solution: Structure and Properties. Adv. Mater. 19 (6) (2007) 821-825. https://doi.org/10.1002/adma.200601521

[22] P. W. Schmidt, S. Morozova, P. M. Owens, R. Adden, Y. Li, F. S. Bates, T. P. Lodge, Molecular Weight Dependence of Methylcellulose Fibrillar Networks. Macromolecules. 51 (19) (2018) 7767-7775. https://doi.org/10.1021/acs.macromol.8b01292

[23] J. Gong, J. Li, J. Xu, Z. Xiang, L. Mo, Research on Cellulose Nanocrystals Produced from Cellulose Sources with Various Polymorphs. RSC Adv. 7 (2017) 33486-33493. https://doi.org/10.1039/C7RA06222B

[24] S. Y. Oh, D. I. Yoo, Y. Shin, H. C. Kim, H. Y. Kim, Y. S. Chung, W. H. Park, J. H. Youk, Crystalline structure analysis of cellulose treated with sodium hydroxide and carbon dioxide by means of X-ray diffraction and FTIR spectroscopy. Carbohydrate Research. 340 (15) (2005) 2376–2391. https://doi.org/10.1016/j.carres.2005.08.007

[25] D. Ye, X. Lei, T. Li, Q. Cheng, C. Chang, L. Hu, L. Zhang, Ultrahigh Tough, Super Clear, and Highly Anisotropic Nanofiber-Structured Regenerated Cellulose Films. ACS nano. 13 (4) (2019) 4843-4853. https://doi.org/10.1021/acsnano.9b02081

[26] F. Vargas-Lara, J. F. Douglas, Fiber Network Formation in Semi-Flexible Polymer Solutions: An Exploratory Computational Study. Gels. 4 (2) (2018) 27.https://doi.org/10.3390/gels4020027

[27] P. W. Schmidt, S. Morozova, S. P. Ertem, M. L. Coughlin, I. Davidovich, Y. Talmon, T. M. Reineke, F. S. Bates, T. P. Lodge, Internal Structure of Methylcellulose Fibrils. Macromolecules. 53 (1) (2020) 398–405. https://doi.org/10.1021/acs.macromol.9b01773

[28] S. E. Szczesny, D. M. Elliott, Interfibrillar Shear Stress is The Loading Mechanism of Collagen Fibrils in Tendon. Acta Biomater. 10 (6) (2014) 2582-2590. https://doi.org/10.1016/j.actbio.2014.01.032

[29] J. Keckes, I. Burgert, K. Frühmann, M. Müller, K. Kölln, M. Hamilton, M. Burghammer,; S. V. Roth, S. Stanzl-Tschegg, Peter. Fratzl, Cell-wall recovery after irreversible deformation of wood. Nat. Mater. 2 (2003) 810–813. https://doi.org/10.1038/nmat1019

[30] D. Zhao, Y. Zhu, W. Cheng, W. Chen, Y. Wu, H. Yu, 2020. Cellulose-Based Flexible Functional Materials for Emerging Intelligent Electronics. Adv. Mater. 2000619, https://doi.org/10.1002/adma.202000619.

[31] B. R. Freedman, D. J. Mooney, Biomaterials to Mimic and Heal Connective Tissues. Adv. Mater. 31 (19) (2019) 1806695. https://doi.org/10.1002/adma.201806695

4.6 Figures

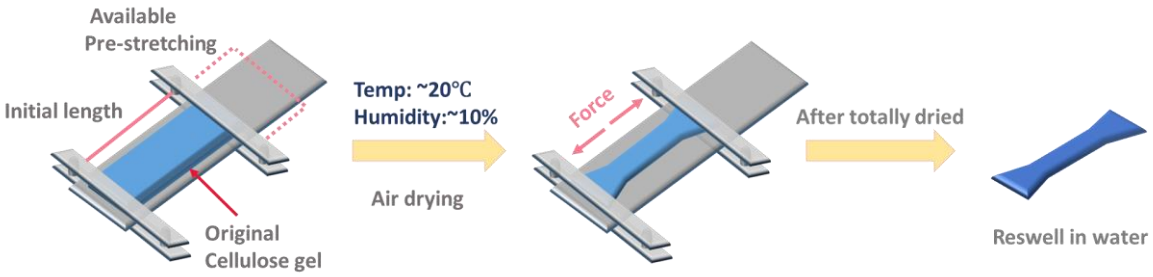

Figure 4.1 Schematic illustration of DCC method.

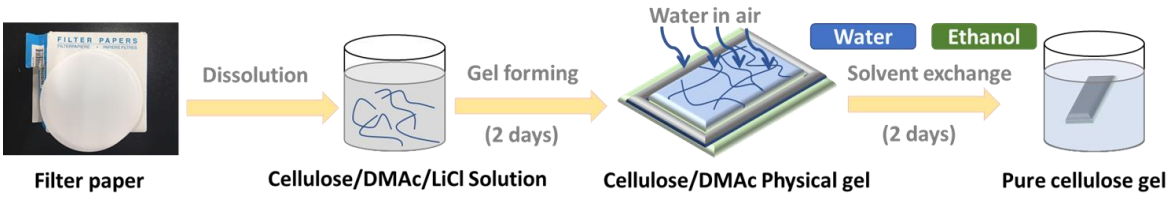

Figure 4.2 Preparation of cellulose gels with DMAc/LiCl solution.

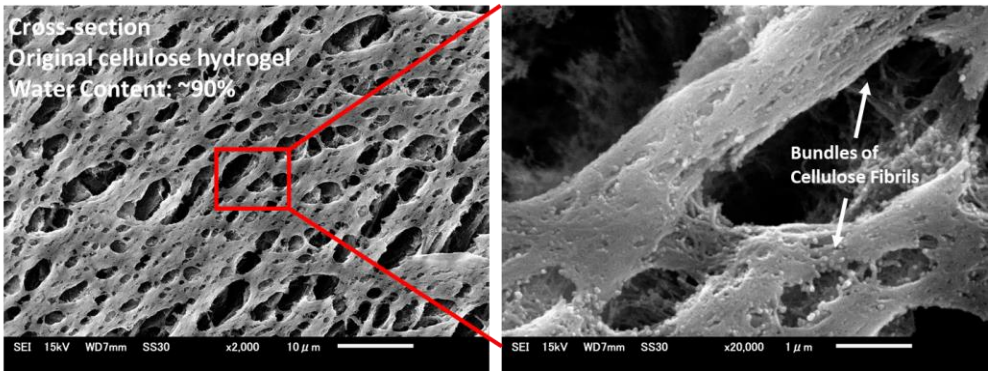

Figure 4.3 SEM observation of cross-section part of original cellulose hydrogel.

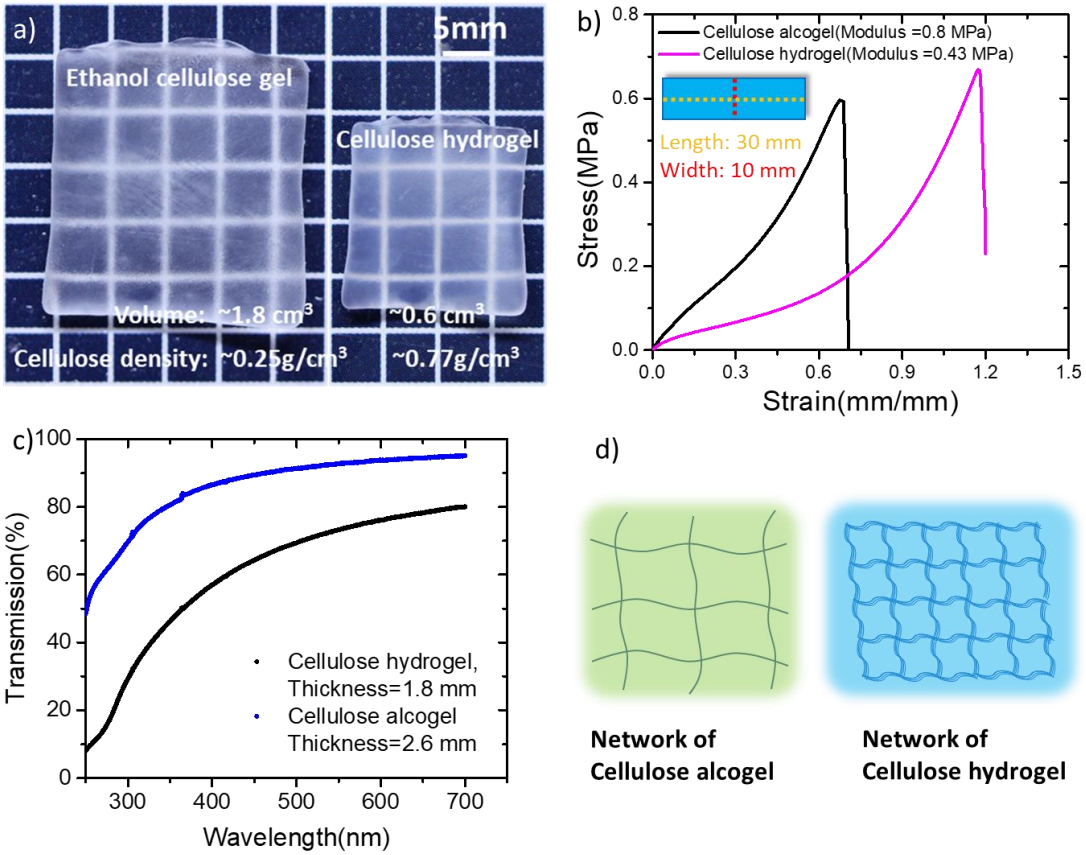

Figure 4.4 Cellulose alcogel and hydrogel compared. a) A photo showing volume difference of the cellulose alcogel and hydrogel prepared with same amount of cellulose. b) Tensile stress-strain curves for the samples cut to 10 mm x 3 mm size (embedded image). c) Optical transmission tests results of the samples. d) Schematic illustrations showing network structures of the cellulose alcogel and hydrogel, where the cellulose hydrogels are made from more aggregated cellulose fibrils.

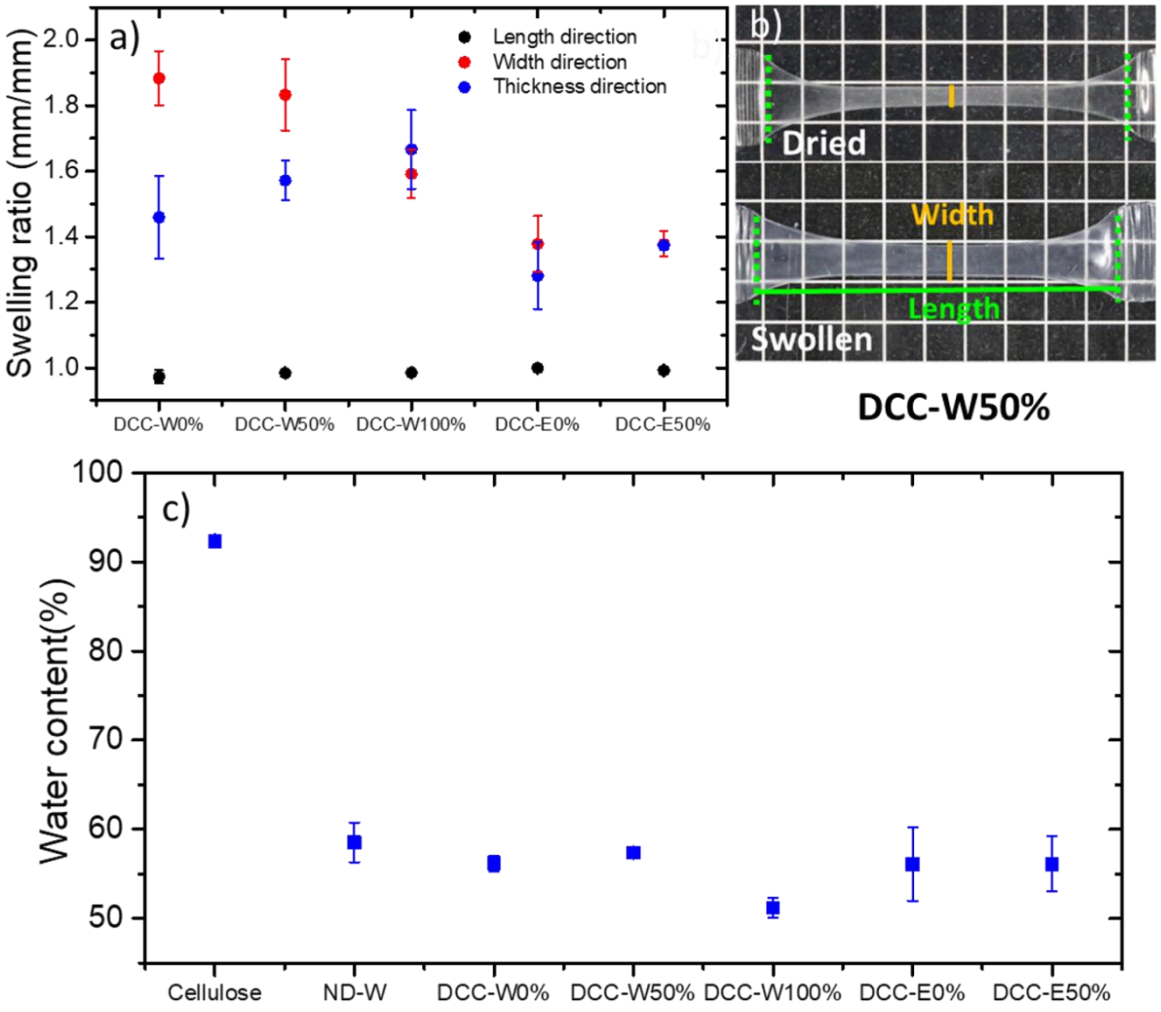

Figure 4.5 a) Swelling ratio in different directions of all DCC samples after immersion in water. b) Digital photos of DCC-W50% samples before and after reswelling in water. c) Water content of original cellulose hydrogel and all DCC samples after reswelling.

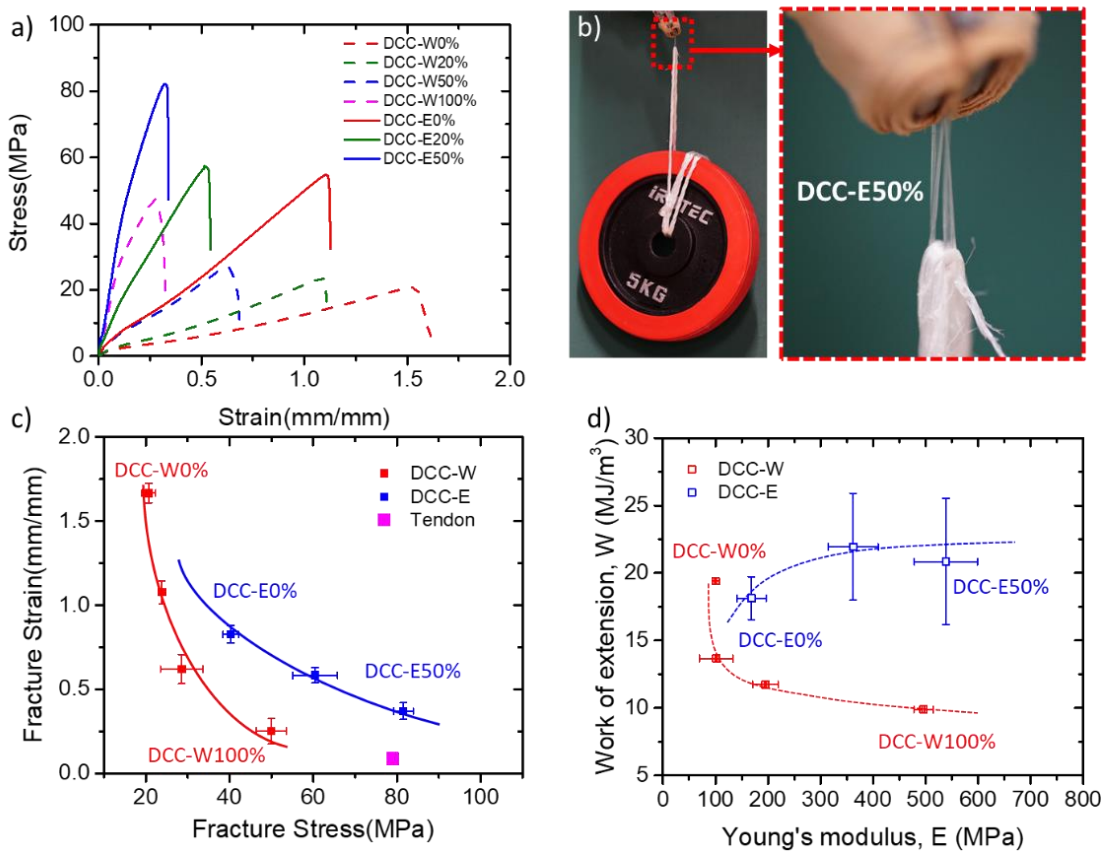

Figure 4.6 a) Tensile stress–strain curves of DCC hydrogels at strain rate of 0.056 s-1. b) Digital photo showing DCC-E50% sample 45 mm long, ~0.5 mm thick, and ~2 mm wide lifted a 5 kg weight. c) Fracture stress-strain curves of DCC samples and human adult tendon; four red dots from high to low fracture strain represent DCC-W0%, DCC-W20%, DCC-W50%, and DCC-W100%, respectively; three blue dots from high to low fracture strain represent DCC-E0%, DCC-E20%, and DCC-E50%, respectively. d) Work of extension as a function of Young's modulus of DCC samples; four red dots from low to high Young's modulus represent DCC-W0%, DCC-W20%, DCC-W50%, and DCC-W100%, respectively;

three blue dots from low to high Young's Modulus represent DCC-E0%, DCC-E20%, and DCC-E50%, respectively.

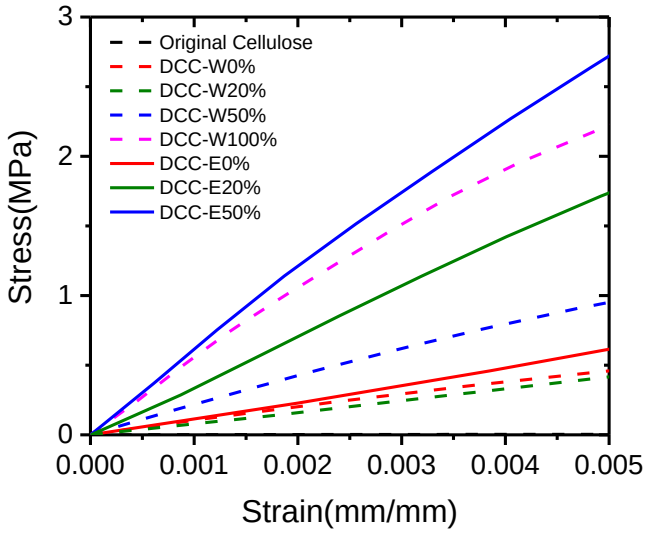

Figure 4.7 Magnification of low region of stress-strain curve.

Table 1. Mechanical properties and water content of different samples prepared under different conditions. Data are compared with a human adult Achilles tendon.

Samples	Sample description	Young's modulus, E (MPa)	Fracture stress, σf (MPa)	Fracture strain, εf (mm/mm)	Work of extension, W (MJ/m3)	Water (wt%)
Cellulose hydrogel	Initial swollen sample	0.43±0.04	0.56±0.1	1.1±0.1	0.21±0.04	92

DCC-W0%	DCC without pre-strain#1	100.33±2.51	20.7±1.61	1.67±0.06	19.4±1.65	56
DCC-W50%	DCC at 50% pre-strain	194.9±24.1	28.6±5.1	0.62±0.09	11.73±1.16	57
DCC-W100%	DCC at 100% pre-strain	496±18.38	50±3.61	0.25±0.08	9.9±2.1	51
Cellulose alcogel	Initial swollen sample	0.8	0.6	0.67	0.18	-
DCC-E0%	DCC without pre-strain	168.67±27.79	40.3±1.85	0.83±0.05	18.13±1.59	56
DCC-E50%	DCC at 50% pre-strain	538.67±60.04	81.53±2.34	0.37±0.05	20.83±4.69	56
Achilles tendon#2	-	~819	~79	~0.088	~3.5	~66

#1DCC: drying under confined conditions

#2Human adult Achilles tendon data from donors aged 35–80 years are shown.[8]

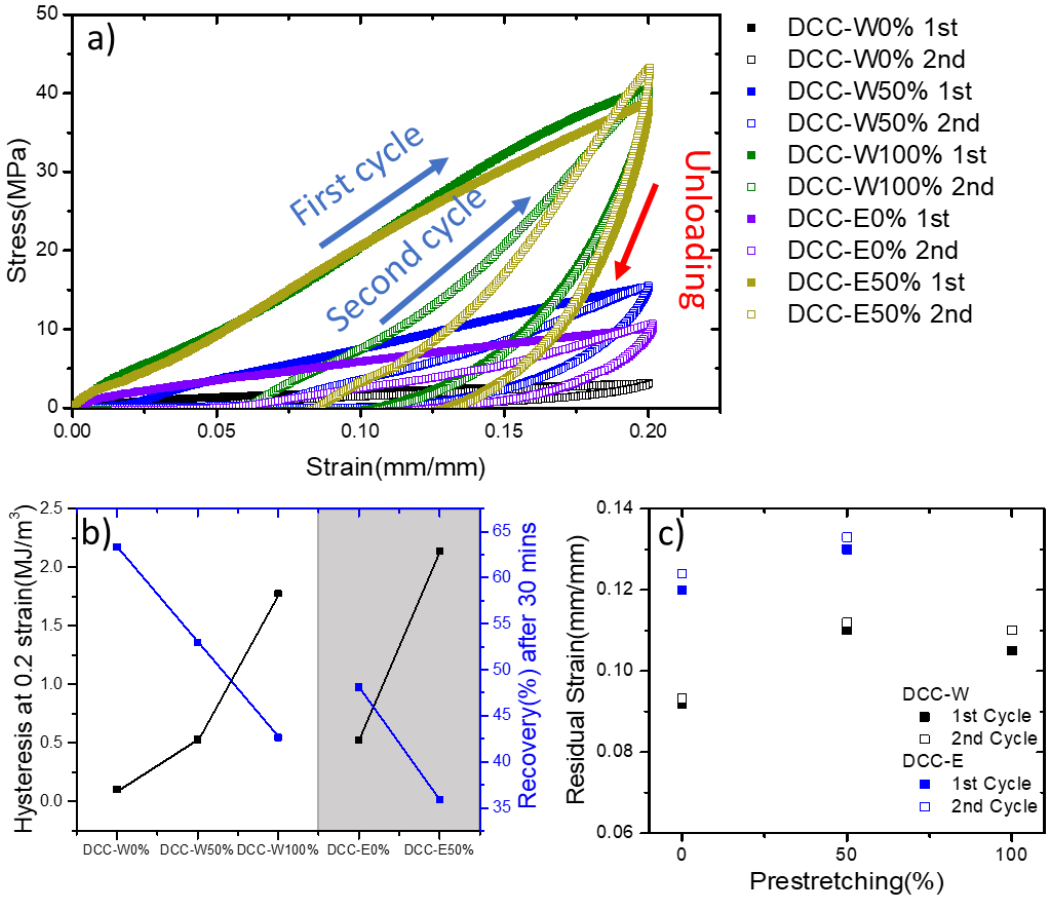

Figure 4.8 a) Cyclic tensile tests up to 0.2 mm/mm strain for all DCC samples at loading and unloading rates of 0.056 s-1. Waiting time between the first and second cycles is 30 min. b) Hysteresis and recovery rate estimated from the ratio of the second hysteresis area to the first hysteresis area. c) Residual strain in the cyclic tests of all DCC samples.

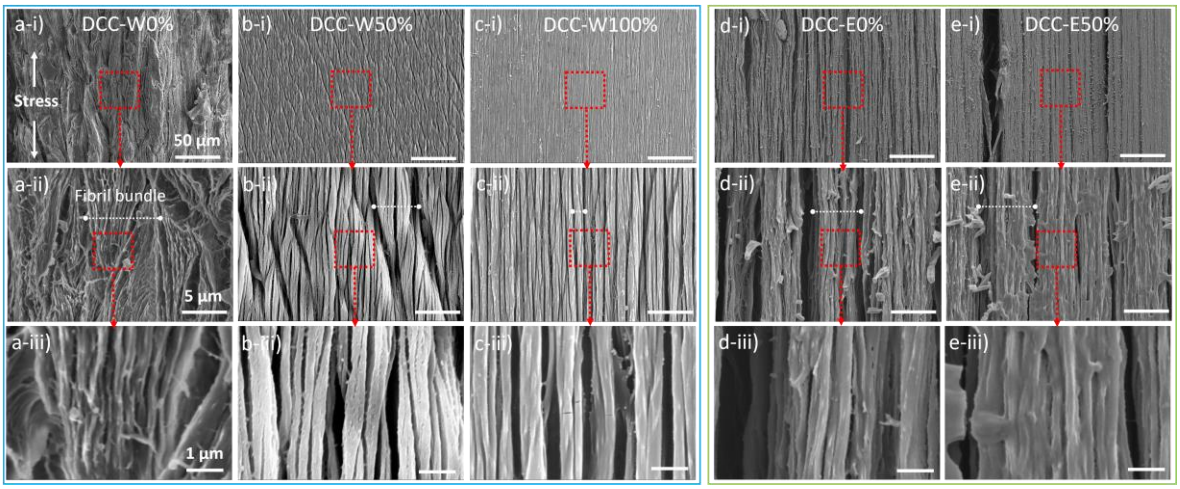

Figure 4.9 SEM images at different magnifications of (a) DCC-W0%, (b), DCC-W50%, (c), DCC-W100%, (d), DCC-E0%, and (e) DCC-E50%. The samples are freeze-dried before observation.

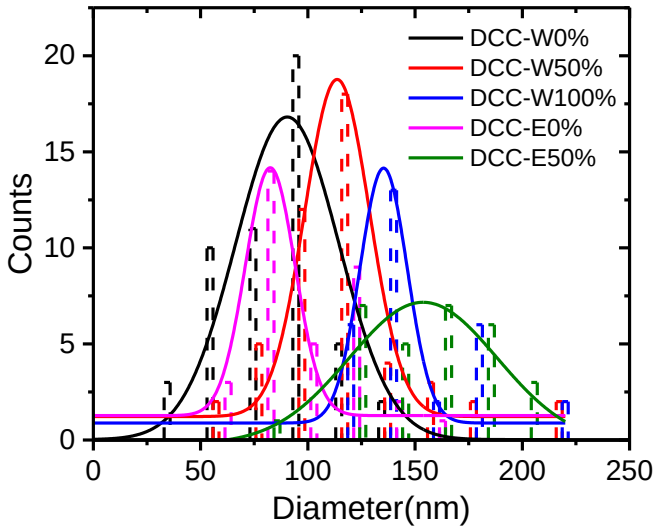

Figure 4.10 Distribution of fibrils' diameter of all DCC samples counted from largest magnification of SEM photos in Figure 8-iii.

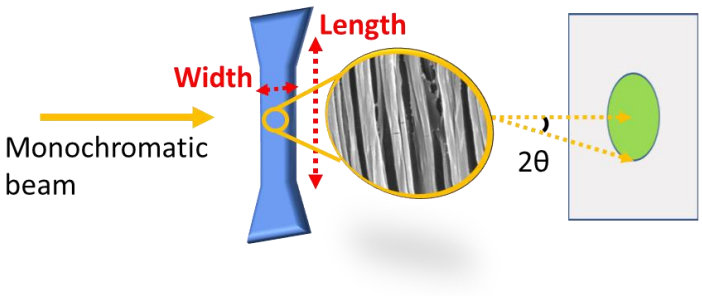

Figure 4.11 Experiment set up of WAXD and SAXS measurements. The DCC stretching direction of samples are in the length direction.

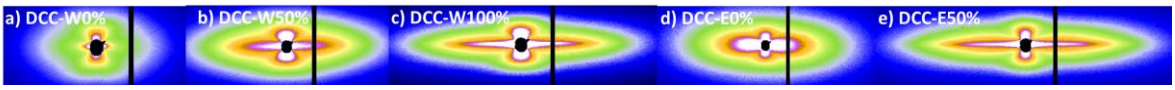

Figure 4.12 Two dimensional (2D) scattering patterns from SAXS of all DCC samples.

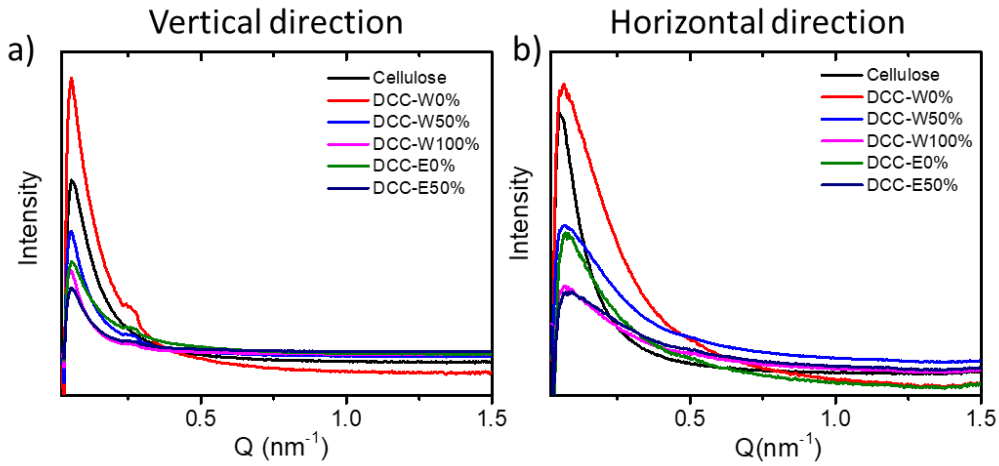

Figure 4.13 Intensity profiles: a) vertical direction, and b) horizontal direction. The size limit of SAXS can be determined using $L = 2\Pi/Q$, where L is the size limit and Q is the position of the beam stop on the x-axis.

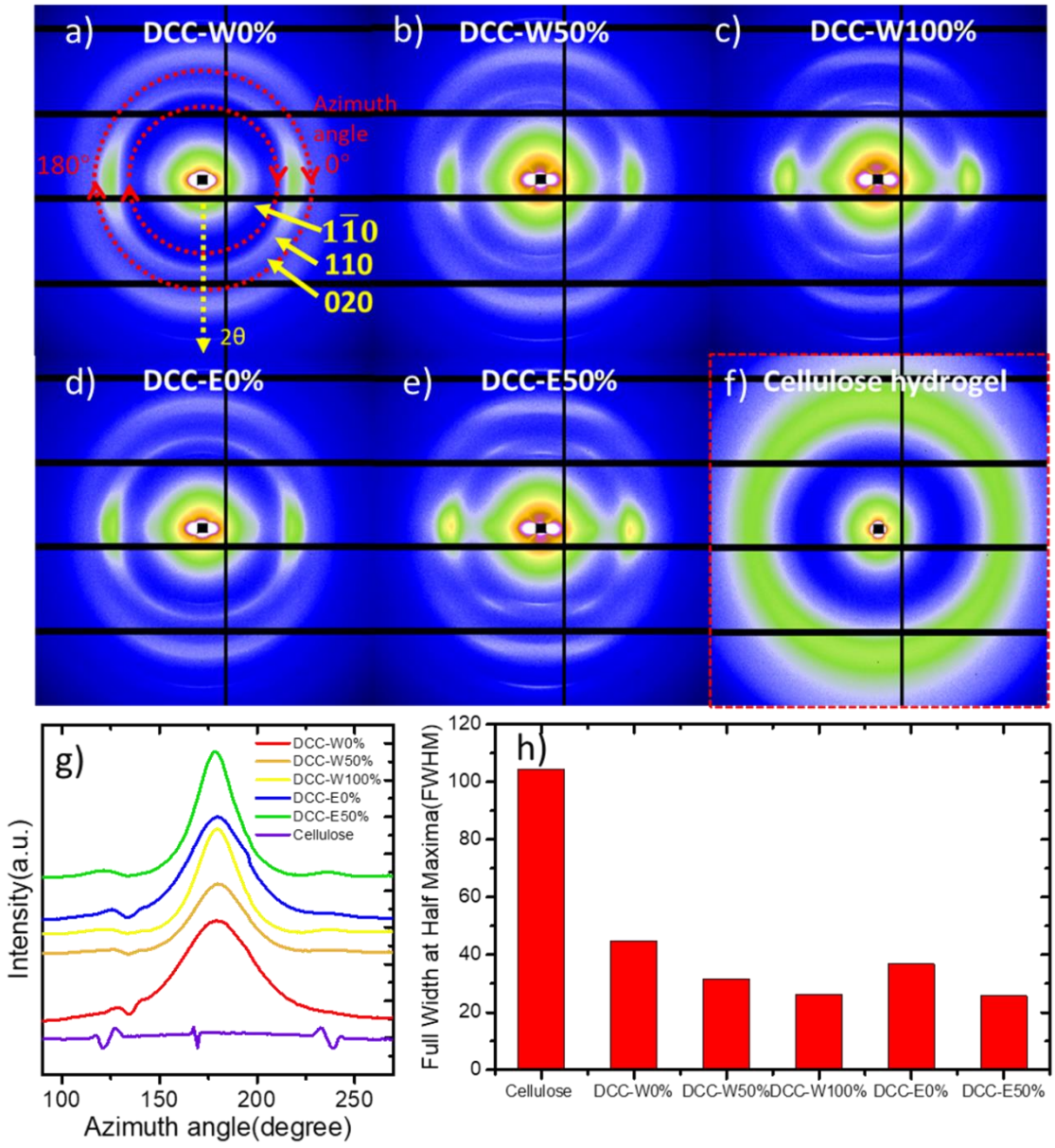

Figure 4.14 a-f) 2D WAXD patterns of DCC samples and cellulose hydrogel. The DCC samples were stretched in the vertical direction. g) Azimuthal-integrated intensity distribution curves for (110) plane of cellulose crystal (scattering angle, 2θ = 20°) of WAXD

pattern, where 180° represents the direction perpendicular to the DCC stretching. h) Full width at half maximum (FWHM) values estimated from the azimuth angle profiles in (g).

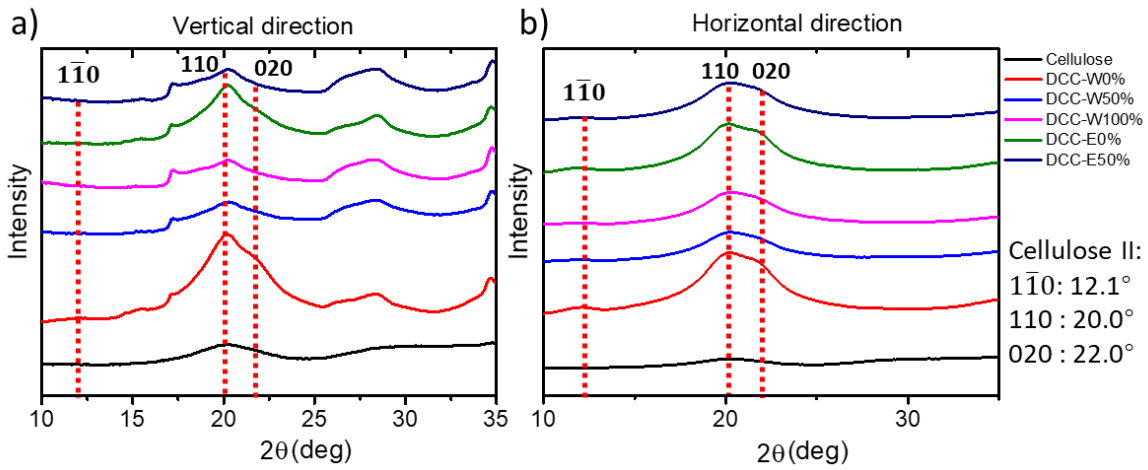

Figure 4.15 Intensity profiles of two directions extracted from 2D WAXD patterns: a) vertical, and (b) horizontal.

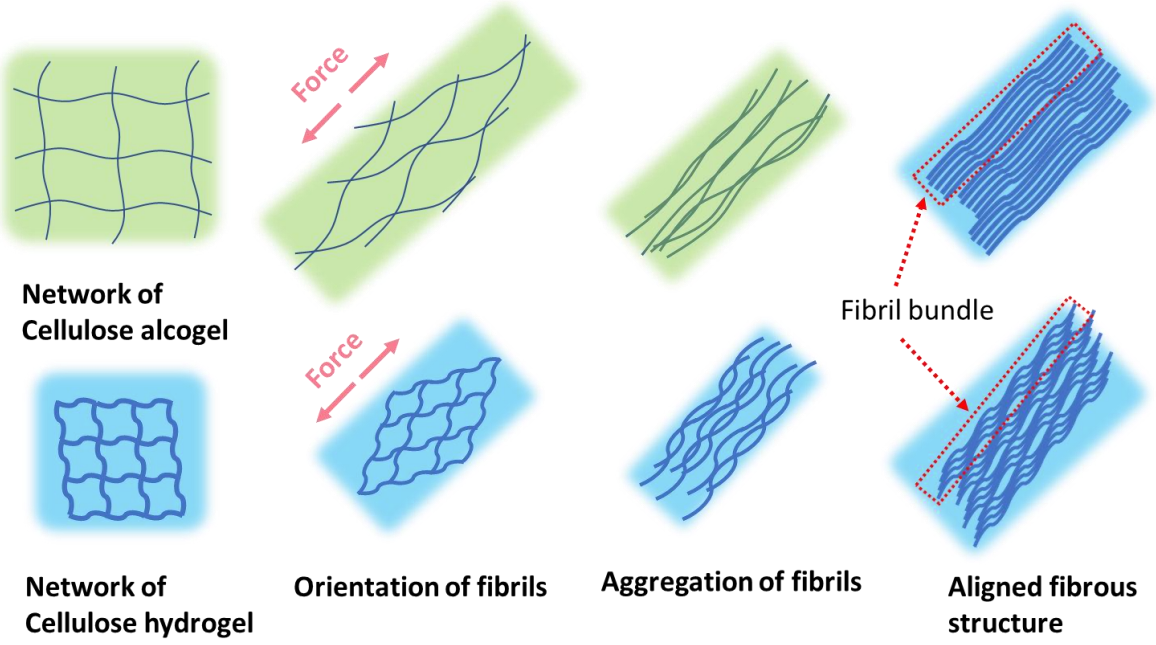

Figure 4.16 Schematic illustration showing different evolving process of fibrous structure for DCC samples prepared from hydrogel and alcogel.

CHAPTER 5

Energy dissipation by multi-scale untwisting of fibrils for DCC-Cellulose hydrogel.

5.1 Introduction

Biological materials are inspiring for hydrogel scientists to prepare tough and strong materials through careful design of hierarchical structure. For example, tendon and ligaments. With highly aligned and hierarchical fibrous structure, those tissue have both high strength and toughness. Mechanism behind this excellent mechanical property is that hierarchical fibrous structure can effectively dissipate the energy while maintain the intact structure. [1]

Previously, we have already confirmed the high toughness and strength of DCC-Cellulose hydrogel. In this chapter, in order to understand the way that hierarchical fibrous structure dissipate the energy, first, we combine cycling tests with SEM observation to analyze the mechanism from structure and energy point of view. And then, by tensile tests with different stretching rate to study the viscoelasticity of DCC-Cellulose samples. Furthermore, SEM observation was also applied to confirm the morphology change. Urea solution was also used in this chapter, with the purpose to undermine the hydrophobic interaction while maintain

the hydrogen bonding between fibrils. The changed energy dissipation behavior and fibrous structure give us more information of the origin of both high toughness and strength of DCC samples.

5.2 Experimental

5.2.1 Materials

Cellulose source (Advantec filter paper, Toyo Roshi Kaisha Ltd., Japan), DMAc and lithium chloride (Tokyo Chemical Industry Co., Ltd, Japan), acetone (Kanto Chemical Co., Inc., Japan) were used as received without further purification. All the aqueous solutions were prepared using ultrapure deionized water.

5.2.2 Gels preparation

Cellulose hydrogels were prepared from filter papers, as previously reported, with some minor difference.[2] The cut filter paper sheets were sequentially washed with water and ethanol. The washed paper was then activated by immersion in DMAc for 12 h and then vacuum dried at 60 °C. To prepare the cellulose solution, 0.75 g activated cellulose was dissolved in 100 g of LiCl/DMAc (8 g: 92 g). The cellulose solution was cast into a glass mold with a thickness of 3 mm. The solution was left in air under ambient conditions (temperature, 20 °C; humidity, 20%). After 2 days, the solution became a weak gel due to the diffusion of water molecules from the air into the cellulose solution. The weak cellulose gel was then placed in pure water and equilibrated for 2 days, changing the water every 12 h, to obtain the cellulose hydrogel (thickness ~2 mm). The cellulose hydrogels were cut into

small pieces 10 mm wide, and 40 mm long and ~2 mm thick, and then loaded into the clamping devices with an initial length between the clamps of 30 mm, as shown in Figure 1. Pre-strains of 0%, 20%, 50%, and 100%, were applied to different samples, keeping them dried at room temperature (humidity 10%–40%) while the length was fixed, to form DCC-Cel 0%, DCC-Cel 50%, and DCC-Cel 100% hydrogels, respectively. After drying for 10 h, all dried samples were removed from the clamping devices and re-immersed in water to obtain the final DCC samples. For comparison, ND-W was also prepared through drying the cellulose hydrogel without any mechanical restriction at room temperature (humidity 10%-40%).

5.2.4 SEM observation

The structures of the samples were characterized by SEM (JSM-6010LA, JEOL Ltd.). To prepare the sample for SEM observation, hydrated samples were freeze-dried using a freeze-drying device (Advantage XL-70, VirTis) and coated with gold using an ion-sputtering device (E-1010, Hitachi, Japan). Changes in the shapes and volumes of the samples were not observed after freeze-drying. In this chapter, to observe the structure change induced by stretch, we conducted liquid nitrogen freezing immediately when a certain sample

5.2.5 Mechanical Characterization

Mechanical property

Tensile tests of gels were conducted in air at room temperature (25 °C) using a commercial mechanical tester (Instron 5965). The tensile speed was 100 mm/min. The distance between the clamps was fixed at 30 mm. Three specimens were used to test each sample. A cyclic

loading-unloading test was carried out in a moist environment to prevent water evaporation, with strain varied as 1%, 2%, 5%, 10%, 20%. In cycling tests of each strain, waiting time was programmed as 0min, 1min, 5min, 20min, 60min, 180min between each cycle. The total cycles is 7 cycles. Stress was defined as the force divided by the initial cross-sectional area of the sample. The fracture stress and fracture strain were defined as the nominal stress and strain at the fracture point, respectively. The Young's modulus E was defined as the value of the initial slope of the stress–strain curve. The work of extension was defined as the area under tensile

5.3 Results and Discussion

5.3.1 Cycling tests.

According to Figure 5.3, DCC-Cel 50% shows large hysteresis in the first cycle, however, from the second loop, only part of the hysteresis is recovered, and the recovered hysteresis show no dependence on waiting time. This part is named as reversible hysteresis, which reflects a fast recoverable structure in DCC-Cel 50%. And the other part of hysteresis is permanently dissipated since first loop, which is called as irreversible hysteresis. The existence of irreversible hysteresis indicate that a large amount of interaction is functioning as sacrificial bonds for DCC-Cel 50%. The structure change is reflected from the residual strain from the cycling tests. As shown in Figure 5.4a, residual strain increase with higher strain in cycling, and the residual strain will keep constant under the cycling tests with the

same strain. As shown in Figure 5.4b, residual strain of first cycle and last cycle under same strain shows no difference.

The hysteresis follows the same regularity with residual strain, as we can see in Figure 5.5a, under the same strain, hysteresis is constant however long the waiting time is. We further plot the change of irreversible hysteresis and reversible hysteresis with different strain. In Figure 5.5b, hysteresis results from DCC-Cel 50% are shown, two different relation are confirmed, irreversible hysteresis shows non-linear increasement with the strain, while reversible hysteresis shows a linear relation with the strain. Then in Figure 5.6, we summarized all the samples' results. The relation between irreversible hysteresis and strain can be well fitted into the equation y=a*X^b, while for reversible hysteresis, the result can be fitted into y=c*X+d. What is the mechanism behind these two equations, and what is the physical meaning of those coefficient. To answer those questions, we conducted quasi-in situ SEM observation on the stretching process of DCC samples.

5.3.2 Structure change during stretching.

As shown in Figure 5.7 and Figure 5.8, the fibrous structure of DCC-Cel 0% can be separated into two areas, twisted area and untwisted areas. In twisted area, fibrils aggregated in a twisted way, while in untwisted area, fibrils adopted a parallel arrangement. Then during stretching process, we confirmed the untwisting behavior of aggregated fibril bundles. As shown in Figure 5.9 and Figure 5.10, the morphology under different strain showing the twisted fibril bundles was gradually elongated to straight fibrils. According to the SEM results, we consider there could be hierarchical twisting area in the fibrous structure, the

twisting area at 10 micron level is the biggest twisting area, which will break first at low strain, we suppose the break of twisting areas will dissipate large amount of energy, and most of which is irreversible. But we don't have enough proof, only judge from the SEM results, fibrils in twisting areas are closely attached together, while in untwisted area, the fibrils loosely distributed, which lack the base for strong interaction. So we suppose the main contribution to the irreversible hysteresis might be the untwisting behavior during stretching, and from the cycling tests, this twisting behavior could exist through the whole process of stretching. In another words, besides the twisting area at 10 microns level, there should be hierarchical twisting area existing in smaller scales. More quantification work needs to be done.

To further prove our hypothesis, we first compared the residual strain of first cycle and last cycle for all samples under different strain, and then we freeze-dried the stretched sample immediately, and observed the structure, compare with the structure in Figure 5.9 and 5.10, the fibrous structure are almost the same, it's hard to give a precise evaluation on the structure change. Here we only want to confirm the fibrous structure has a permanent damage after being stretched.

Above discussion focused on DCC-Cel 0%, and we try to confirm the structure change in all DCC samples. As shown in Figure 5.14, stretched fibrous structure show no obvious change after waiting 10 minutes in water.

5.3.3 Cycling tests under different stretching rate

Figure 5.16 summarized the results from cycling tests with different stretching rate, as we can see in Figure 5.16a, the irreversible hysteresis shows very limited rate dependence, while the reversible hysteresis shows a relative larger slope, but the viscoelasticity is still very limited. Take a closer look at the hysteresis results. First, for the irreversible hysteresis, even for the original cellulose hydrogel, the irreversible hysteresis is very low. As we previously revealed, the fibrous structure has already formed in original cellulose hydrogel, but not as dense as the DCC samples, the possible reason might be that the cross-linking between fibrils is irreversible, the hydrophobic interaction drives the close attachment of molecules or fibrils, it will lay a solid foundation for formation of abundant hydrogen bonding, because the hydroxy groups on cellulose are so close, they prefer to form inter-molecular hydrogen bonding rather than interacting with water molecules. [ref] Hence, when we break the cross-linking between fibrils, the hydrogen boding will be broken, the hydrophobic part of cellulose will be exposed. Under this circumstances, the broken cross-linking is unable to form again, because the existence of other cross-linking limited the flexibility of molecules or fibrils. And as for the reversible hysteresis, the main contribution to which should be hydrogen bonding between the fibrils. while these hydrogen bonding should be mainly exist in fibril bundles, but not the cross-linking area. When the hydrogen bonding was broken by stretching, they form again when the stretching force is removed.

5.3.4 DCC samples in urea solution

Urea solution can be used for studying the interaction between fibrils. Urea molecules can undermine the hydrophobic interaction while maintain the hydrogen bonding, [ref] as shown in Figure 5.18.

After immersed in Urea solution for 12 hours, the volume of cellulose hydrogels reached equilibrium. We first measured the anisotropic swelling ratio of DCC samples. Compare with normal DCC samples. as we can see in Figure 5.19, the UDCC samples show no obvious change in swelling ratio. And then we did tensile tests for UDCC samples, the result is presented with previous normal DCC samples together. As shown in Figure 5.20, the UDCC samples show decreased fracture stress, while the fracture strain maintained the same level with DCC samples. In Figure 5.21, we summarized the modulus results, the modulus shows obvious decline for UDCC samples. And the change of fracture stress and fracture strain are conform to the tensile results.

In our previous study, we confirmed that the interaction between fibrils and the orientation degree are all very important to the young's modulus. And in this study, urea cellulose shows no obvious volume change in urea solution, and UDCC samples also shows no obvious swelling ratio change in all directions, so we consider the main reason for declined young's modulus is the weakened interaction between fibrils. To confirm this assumption, we further did cycling tests to check the energy dissipation behavior of UDCC samples. As shown in Figure 5.22, 2 cycles for each UDCC samples, and UDCC samples also show 2 different hysteresis, the large irreversible hysteresis and reversible hysteresis of second cycle. We

summarized all result from cycling tests, as we can see in Figure 5.23, all hysteresis of UDCC samples show an obvious decline compare with original DCC samples. Combine SEM observation with above results will give us a better understanding of the mechanical property of cellulose hydrogel. In Figure 5.24, the fibrous structure of UDCC samples are loosely crosslinked between each other compare with corresponding DCC samples, the urea solution surely undermined the hydrophobic interaction between fibrils and makes fibrils start to separated, the lower crosslinking density might be a important reason for the decline of young's modulus. And in Figure 5.25, after 0.2 strain, in UDCC samples, more smaller fibrils are exposed, but those separated fibrils seem to be still inter-connected with each other, those connected fibrils are the reason that even the fracture stress shows an obvious decline due to the low cross-linking density, the fracture strain can still maintain in the same level with original DCC samples. We consider that the cross-linking points in UDCC fibrous structure are strong interaction which might be covalent bonding in the form of ester linkage.[ref] And there are also abundant weak interaction between fibrils function as cross-linking points, those weak interaction could be broken by urea solution.

5.4 Conclusion

In this chapter, we confirmed the irreversible hysteresis and reversible hysteresis by cycling tests, and through quasi in situ SEM observation, we confirmed that the untwisting behavior of fibrous structure. Twisted area might contribute large amount of energy to total hysteresis,

and most of which might be irreversible. More quantification work needs to done for confirmation.

By doing cycling tests with different stretching rate, we found that cellulose samples show very limited viscoelasticity, and by fitting the results from irreversible hysteresis and reversible hysteresis we found that reversible hysteresis shows a larger viscoelasticity compare with irreversible hysteresis. And by using urea solution to undermine the hydrophobic interaction between cellulose fibrils we found that hydrophobic interaction plays an important role in both irreversible hysteresis and reversible hysteresis. Combine the SEM observation, we found that there could be 2 different kinds of cross-linking between cellulose fibrils, one is strong interaction which is hard to break though immersion in urea solution, another one is weak interaction which could be broken though urea solution, and make the cellulose fibrils separated. Quantify work need to be done to research interaction between fibrils, urea solution with different concentration will be used to further check the resulted change in mechanical performance.

5.5 References

[1] Spencer E. Szczesny, Dawn M. Elliott, Interfibrillar shear stress is the loading mechanism of collagen fibrils in tendon, Acta Biomaterialia, 10, 6, 2014, 2582-2590, https://doi.org/10.1016/j.actbio.2014.01.032.

[2] M. T. I. Mredha, Y. Z. Guo, T. Nonoyama, T. Nakajima, T. Kurokawa, J. P. Gong, A Facile Method to Fabricate Anisotropic Hydrogels with Perfectly Aligned Hierarchical

Fibrous Structures. Adv. Mater. 30 (9) (2018) 1704937. https://doi.org/10.1002/adma.201704937

5.6 Figures

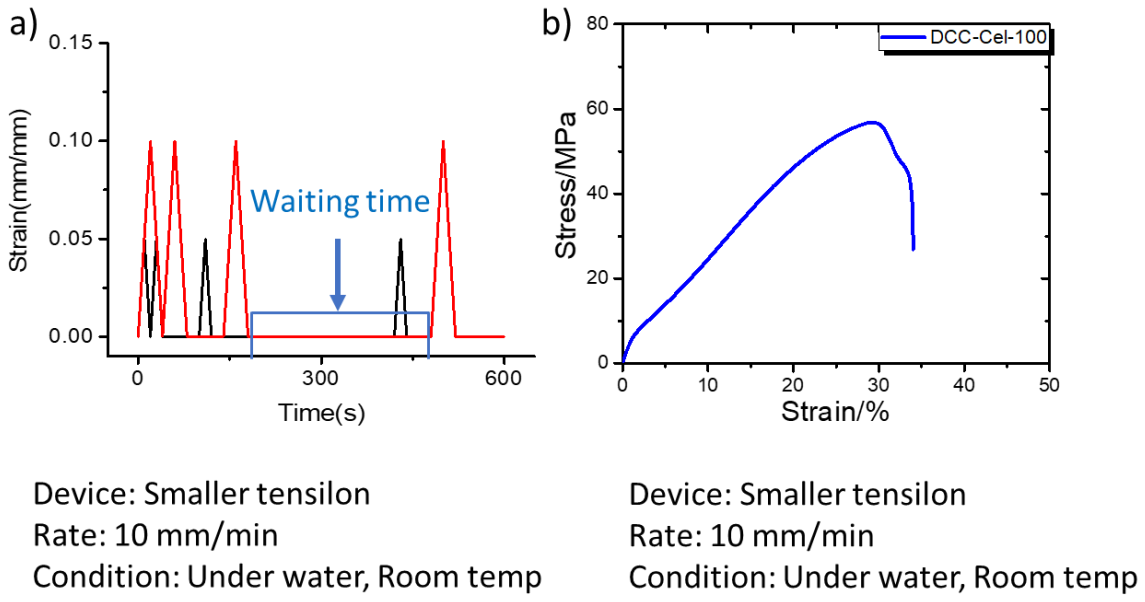

Figure 5.1 a). Experimental design of cycling test. b). Conduct freezing dry treatment at different strain for SEM observation.

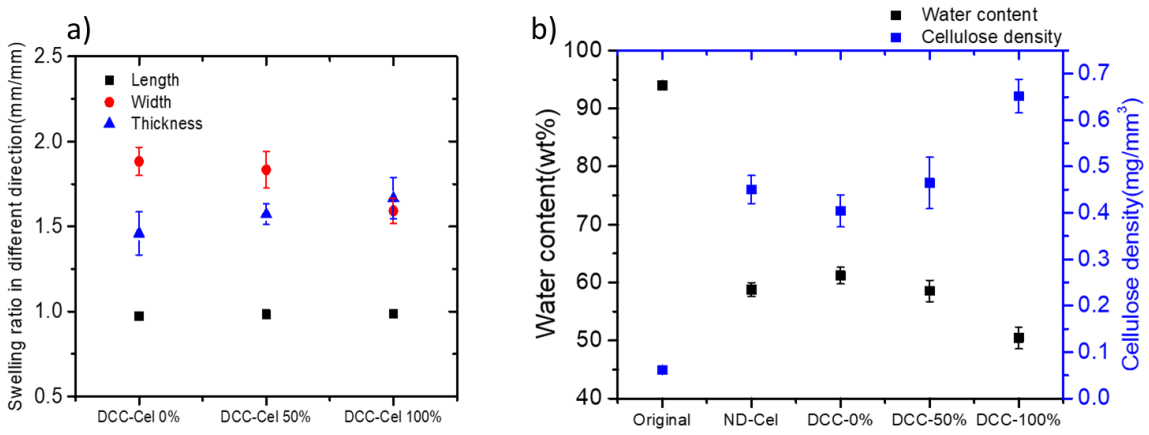

Figure 5.2 a) Swelling ratio of different directions of DCC samples. b). Water content and cellulose density of all samples.

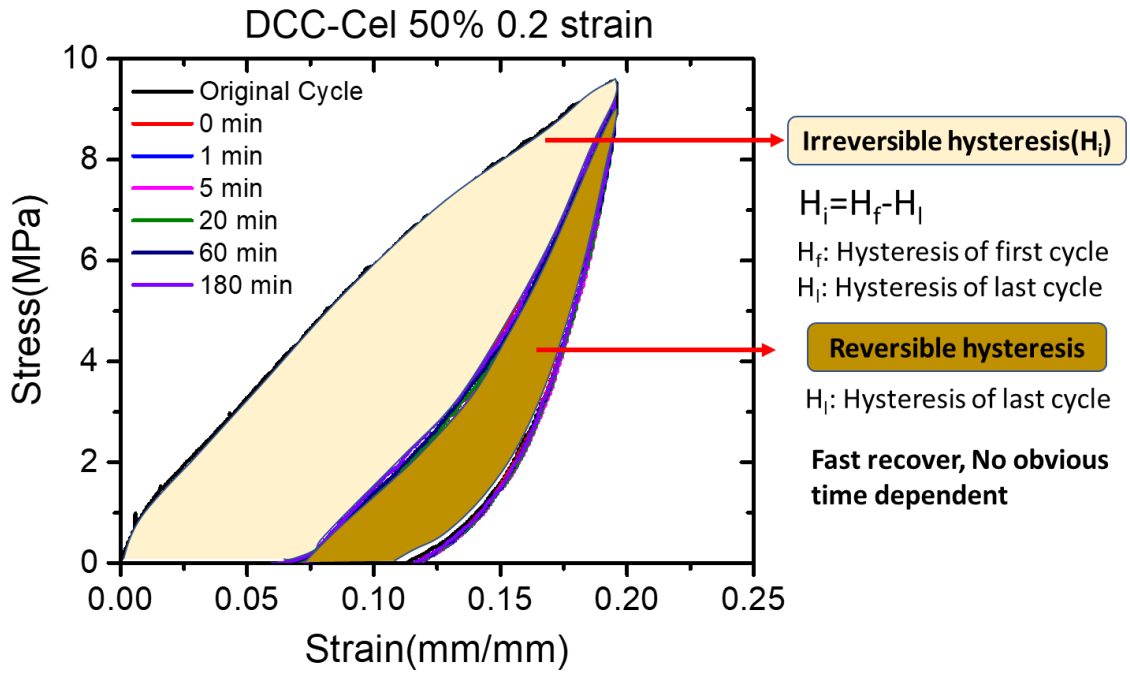

Figure 5.3 Illustration of two different hysteresis during cycling test.

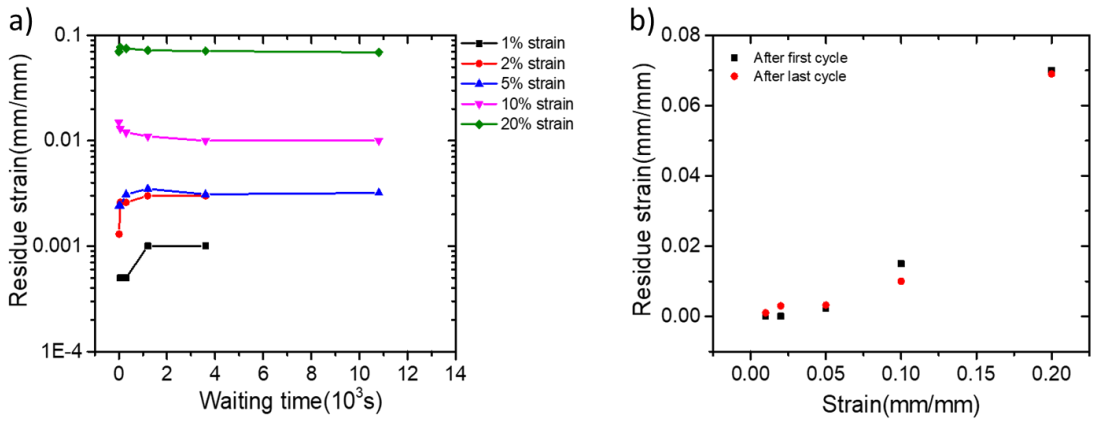

Figure 5.4 a). Residue strain of DCC-Cel50% at different strain. b). Residue strain of DCC-Cel 50% of first cycle and last cycle.

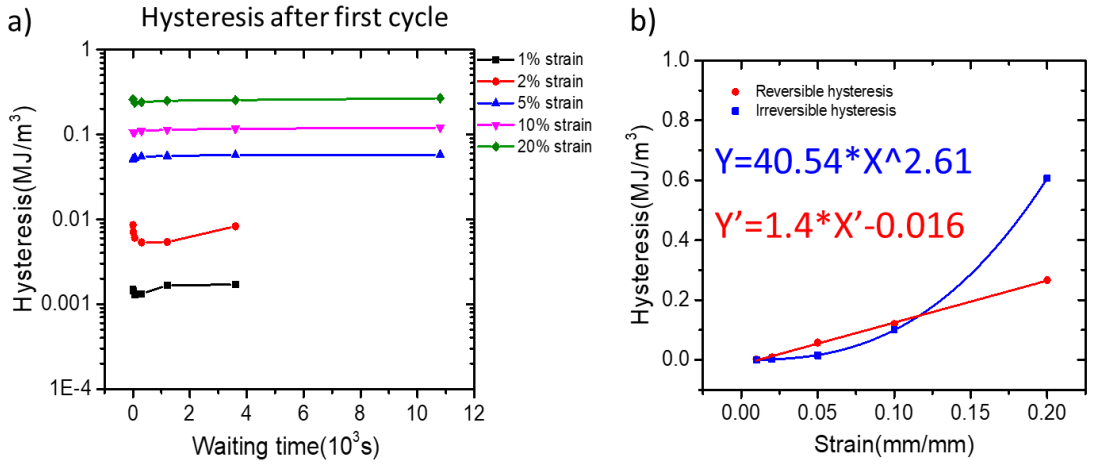

Figure 5.5 a). Total hysteresis of DCC-Cel 50% after different cycles and different waiting times. b). For DCC-Cel 50%, the relation between hysteresis and cycling strain value.

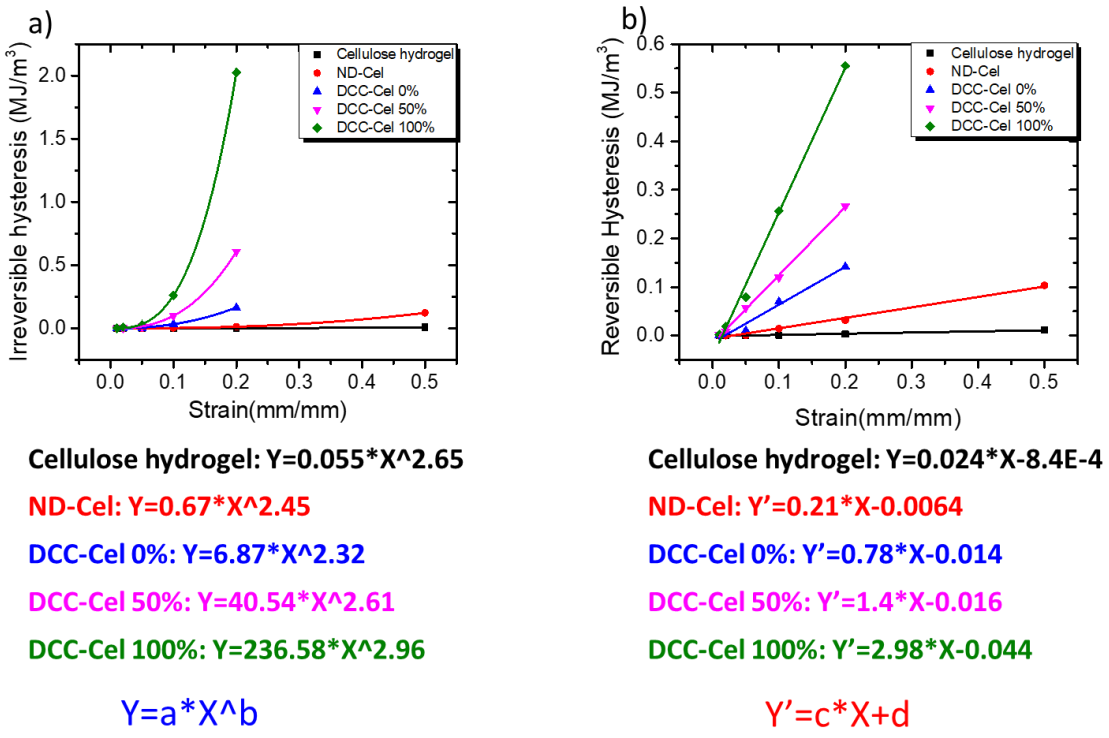

Figure 5.6 a). For all the samples, the relation between irreversible hysteresis and cycling strain. b). For all samples, the relation between reversible hysteresis and cycling strain.

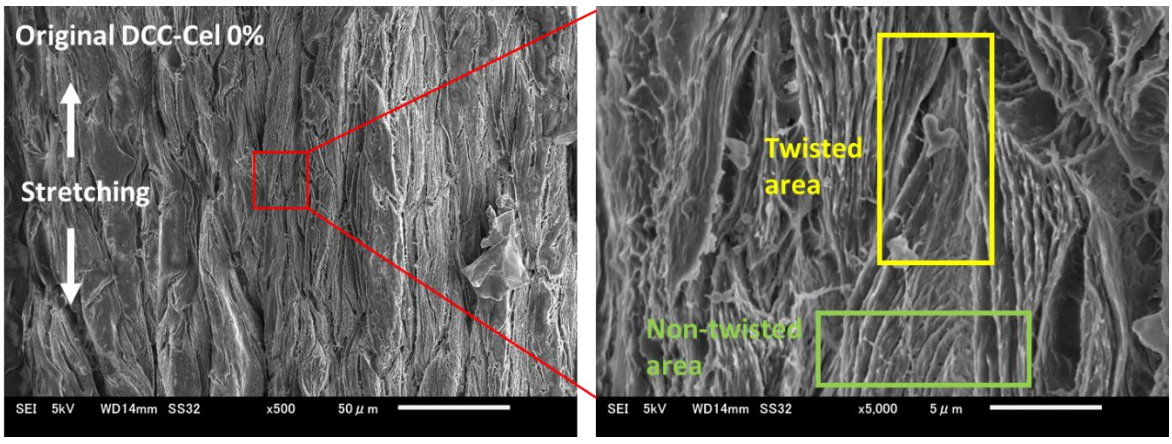

Figure 5.7 SEM observation on the surface of DCC-Cel 0% under different magnification.

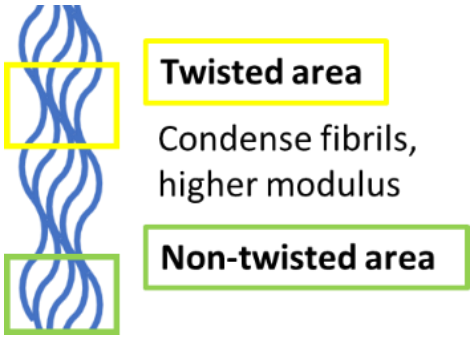

Figure 5.8 Schematic showing possible fibrils arrangement of DCC-Cel 0%.

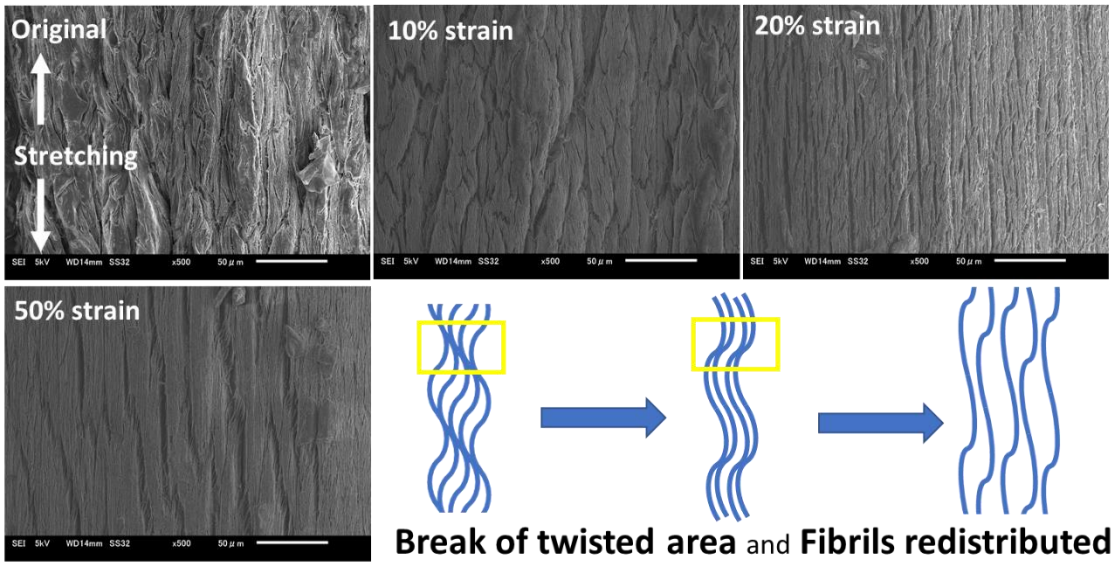

Figure 5.9 Structure evolution of DCC-Cel 0% under stretching.

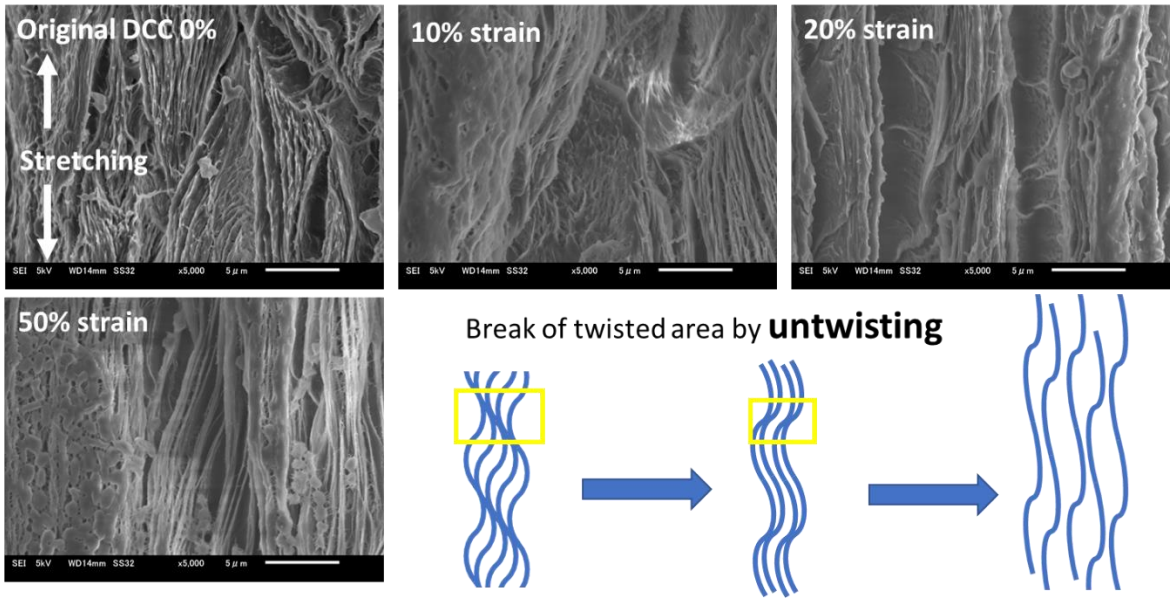

Figure 5.10 Structure evolution DCC-Cel 0% under higher magnification.

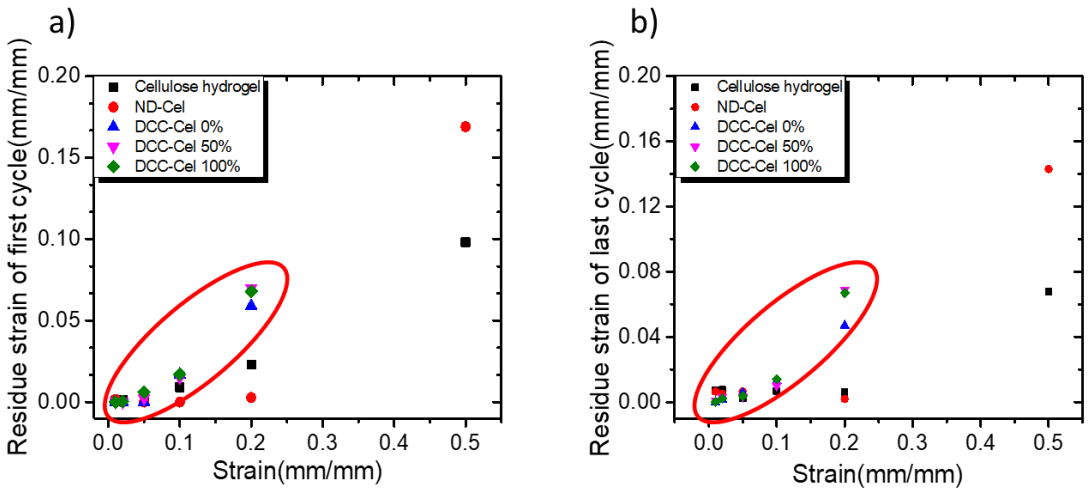

Figure 5.11 a). Residue strain of first cycle of all samples. b). Residue strain of last cycle of all samples.

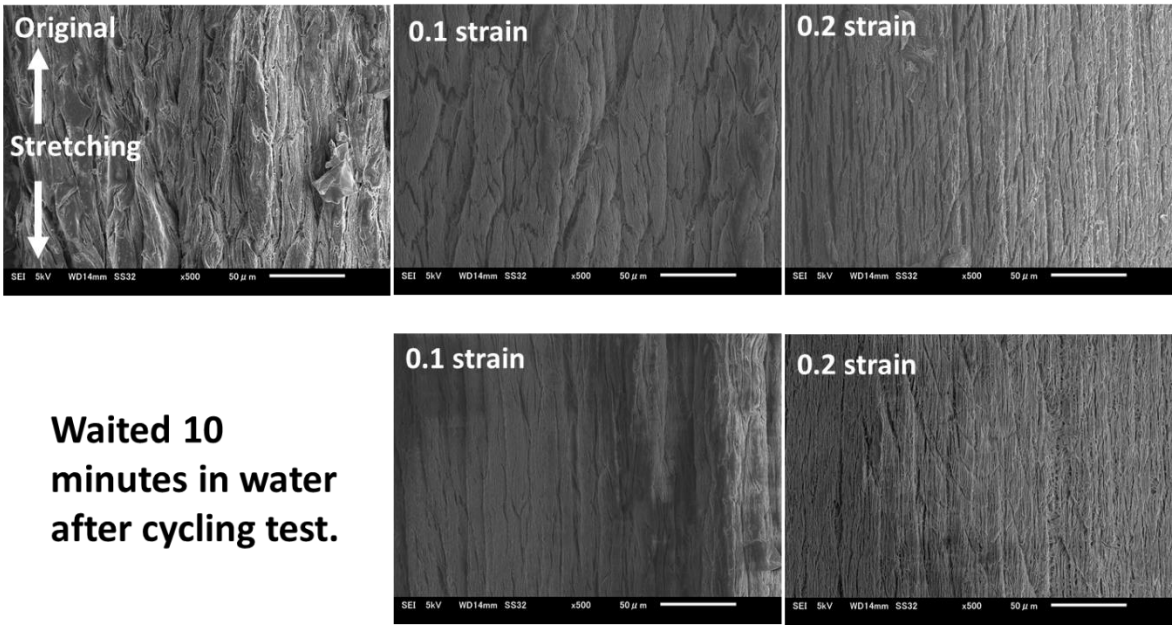

Figure 5.12 SEM observation on DCC-Cel 0%, after being stretched to a certain strain and then immersed in water for 10 minutes.

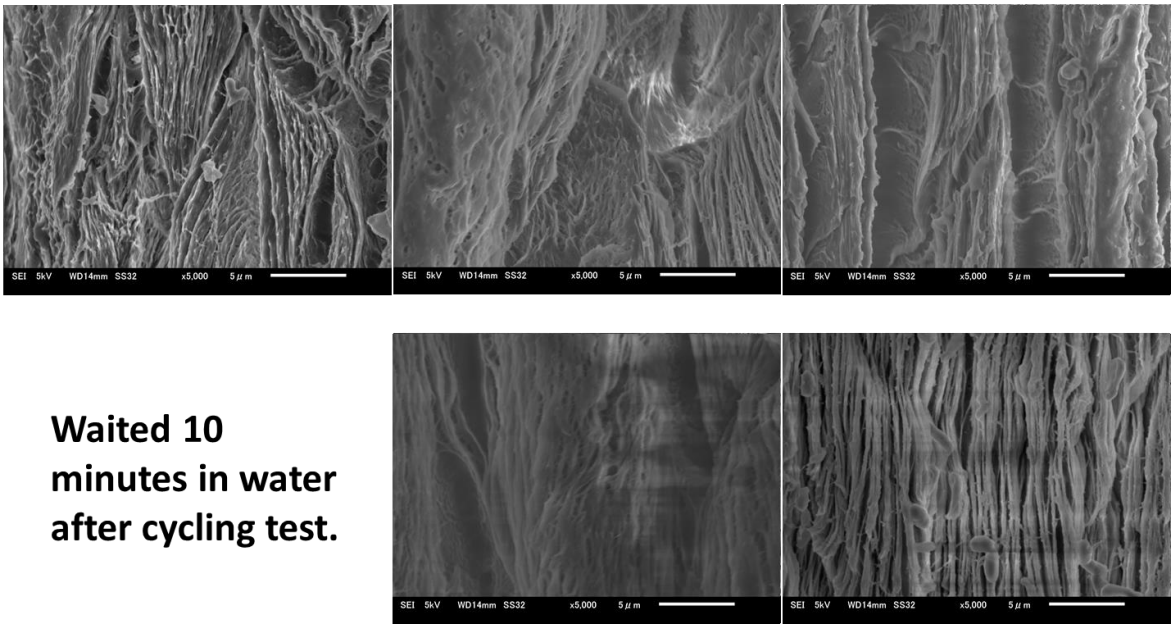

Figure 5.13 Magnification of previous SEM photos.

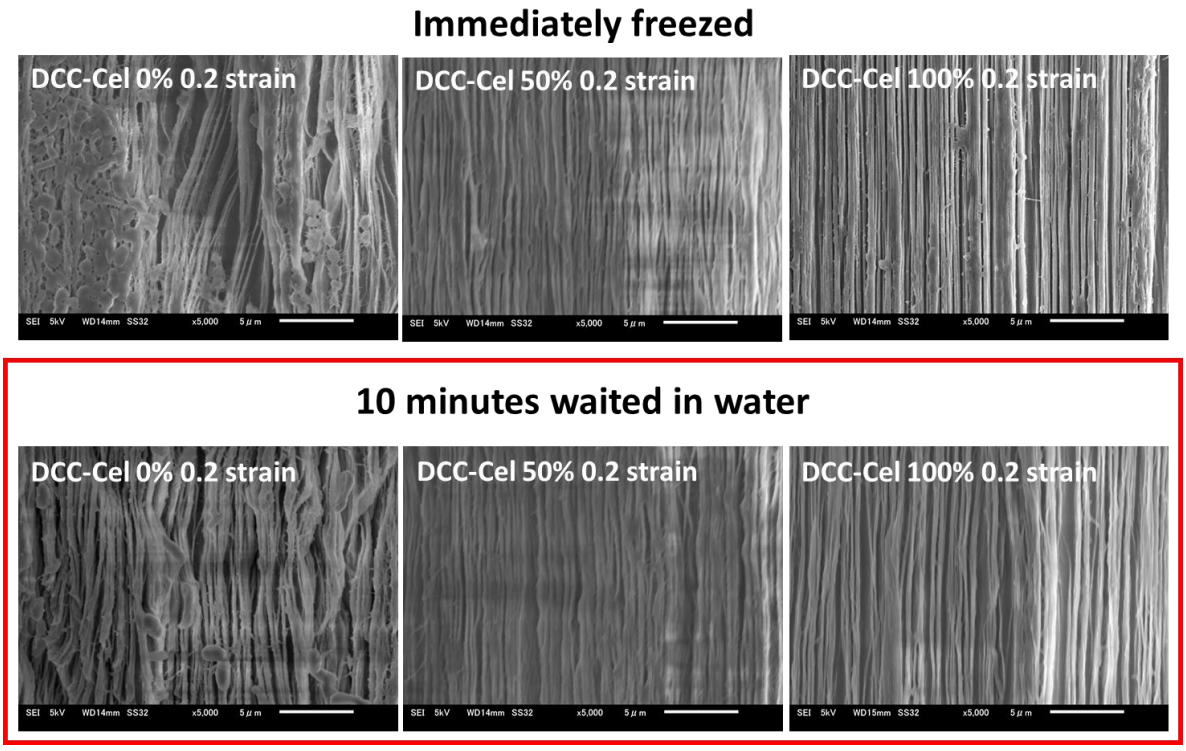

Figure 5.14 SEM observation on DCC samples with different prestretching after being stretched to 0.2 strain. Upper photos showing the structure of immediately freezed sample. Lower photos showing the structure of samples waited in water for 10 minutes.

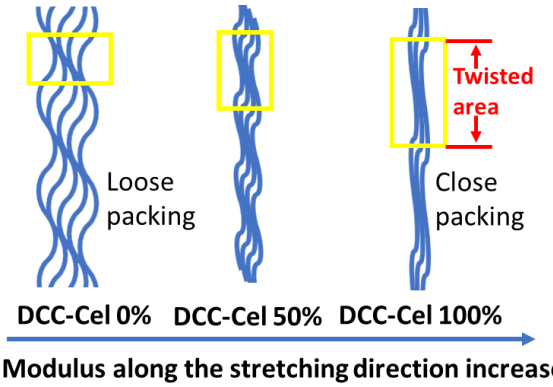

Figure 5.15 Schematic showing the different fibril bundles in different DCC samples.

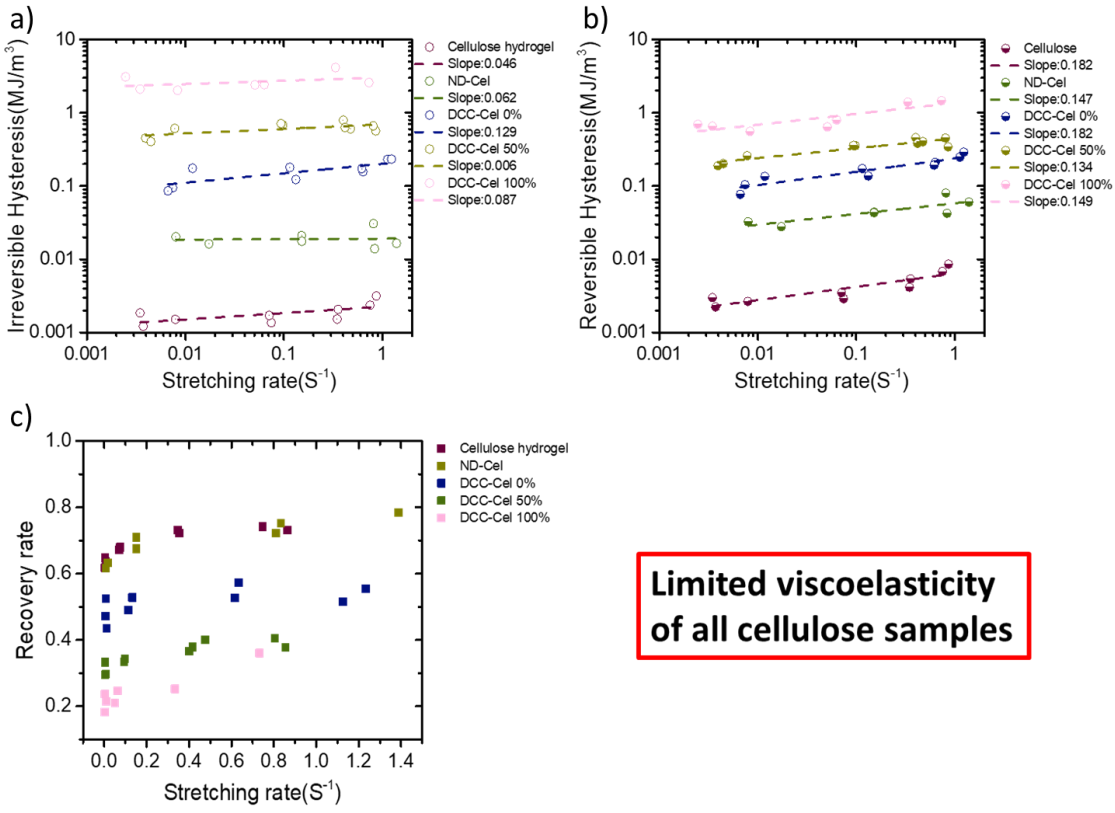

Figure 5.16 For all cellulose hydrogel samples. a) Relation between irreversible hysteresis and stretching rate. b) Relation between reversible hysteresis and stretching rate. c) Relation between recovery rate and stretching rate.

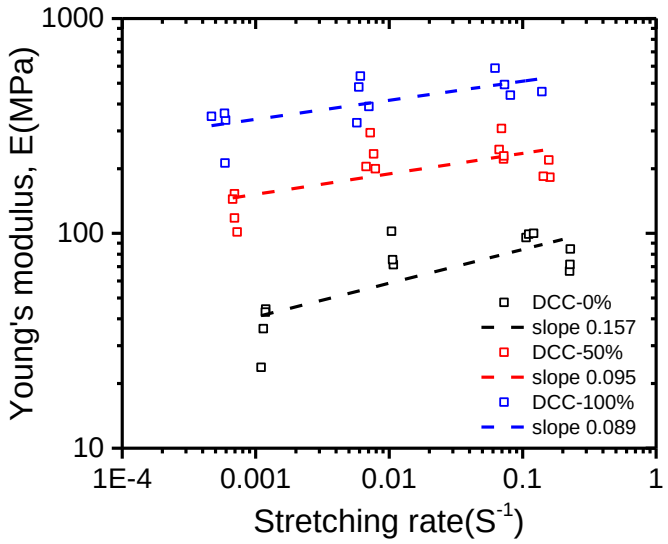

Figure 5.17 For DCC samples, the relation between young's modulus and stretching rate.

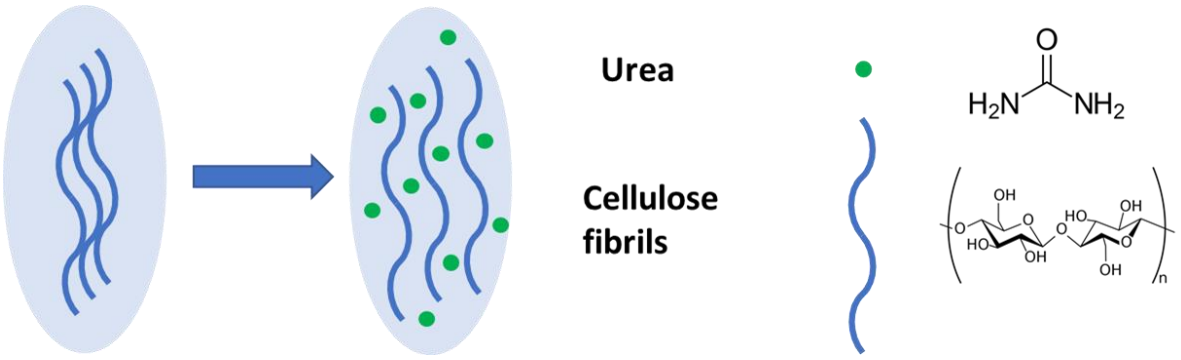

Figure 5.18 Schematic illustration of interaction between cellulose fibrils in urea solution.

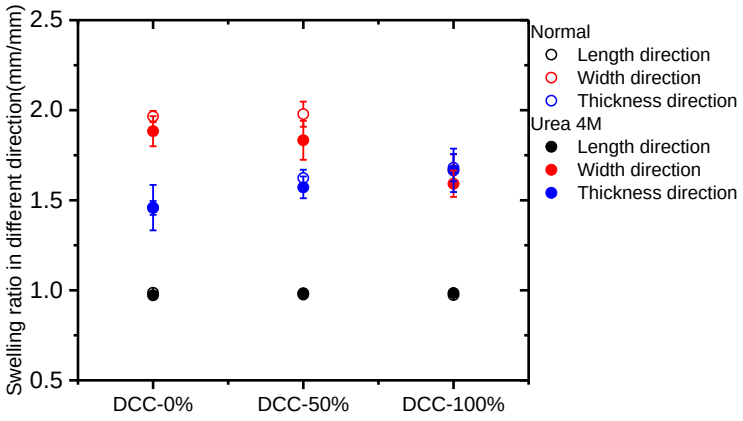

Figure 5.19 Anisotropic swelling behavior of DCC samples in water and urea solution.

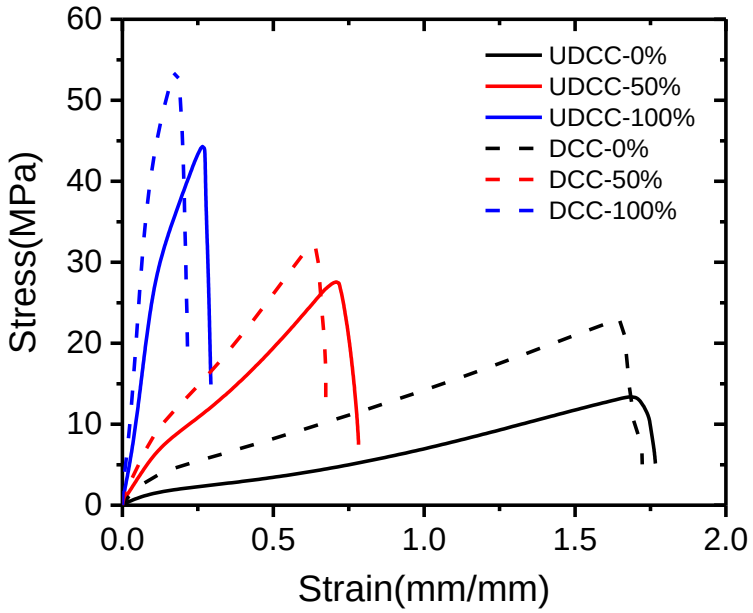

Figure 5.20 Tensile tests of DCC samples and UDCC samples.

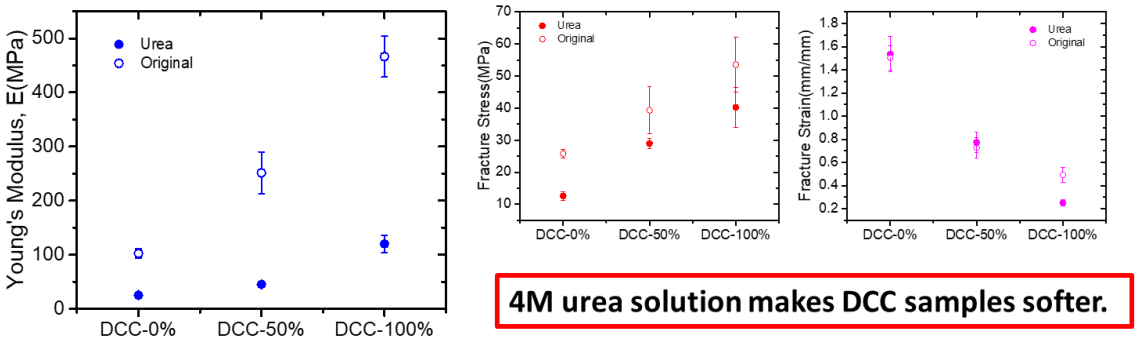

Figure 5.21 Summary of tensile tests.

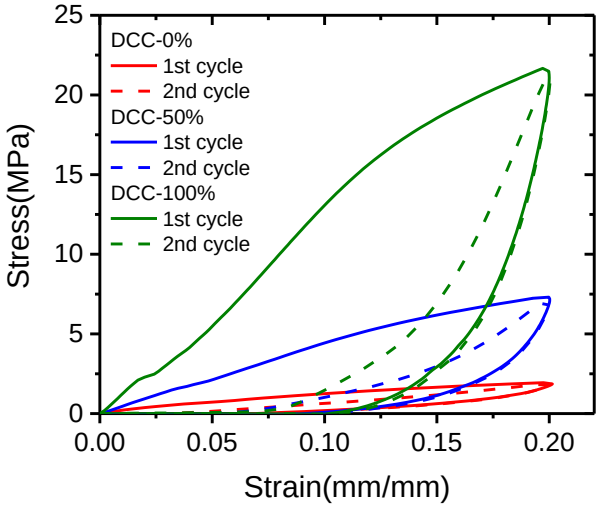

Figure 5.22 Cycling tests for UDCC samples.

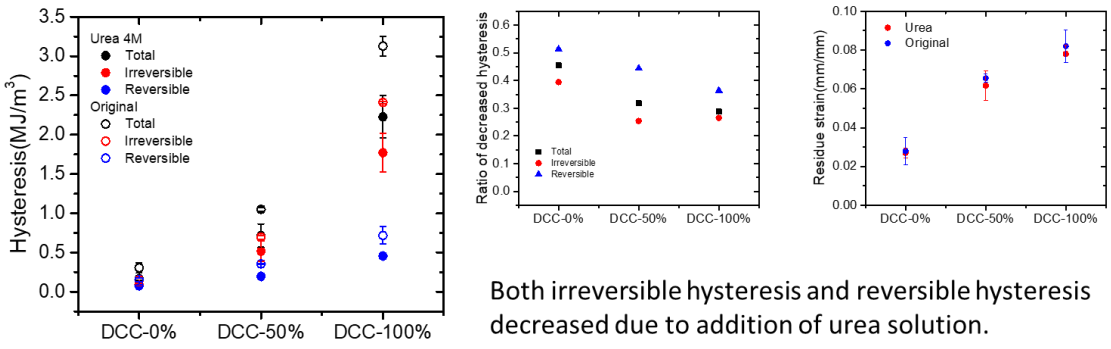

Figure 5.23 Summary of cycling tests for DCC and UDCC samples.

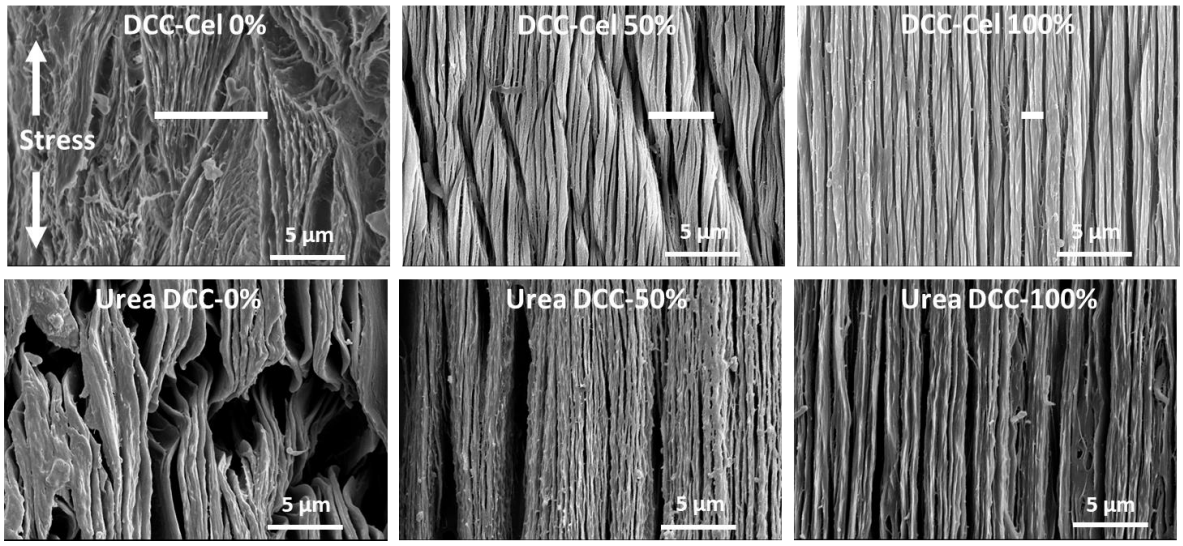

Figure 5.24 Fibrous structure comparison between DCC and UDCC samples.

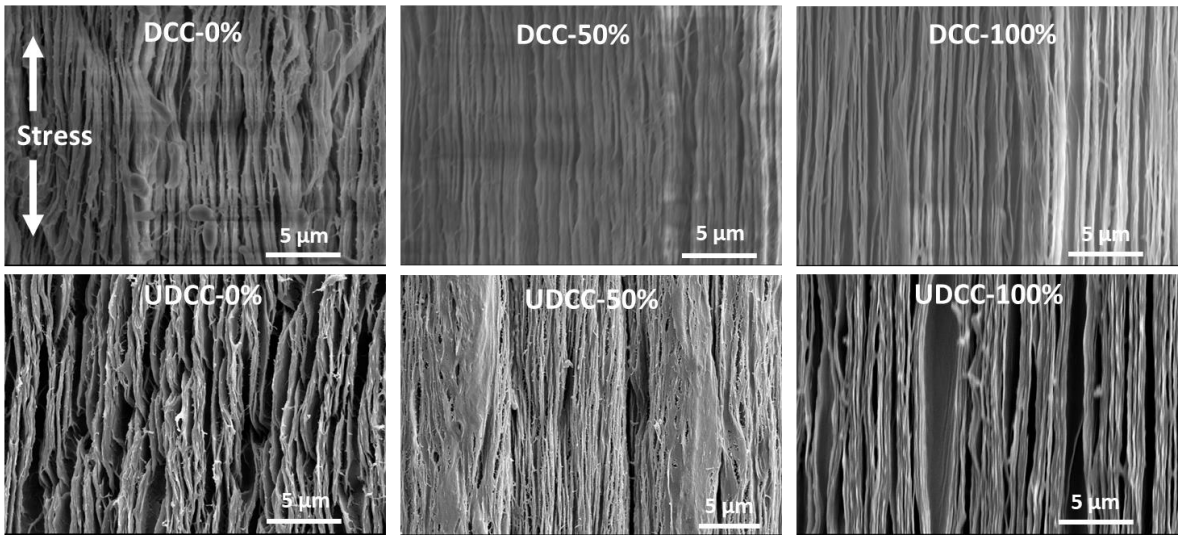

Figure 5.25 After cycling test (0.2 strain), the comparison of fibrous structure between DCC and UDCC samples.

CHAPTER 6

Training cellulose hydrogel through DCC method.

6.1 Introduction

Biological load-bearing tissues are dynamic, open systems in which structural transformations to adapt surrounding mechanical environment are constantly occurring through metabolic processes. Specifically, skeletal muscles hypertrophy and strengthen due to the repeated exercise. The destruction of fibrous structure is caused by exertion, whereas the supply of building blocks such as amino acid and constructive chemical reactions grows new muscle. Similar phenomenon can also be observed in plants which mainly consists polysaccharides like cellulose and alginate. [1] For example, trees grow in the blustery places will bend along the wind wind direction, and many other phenomenon also reflects that polysaccharides can also adapt to surrounding forces.

Those biological materials are inspiring for hydrogel scientists to prepare dynamic hydrogel system which can adapt to surrounding forces. Previously in our lab, we have developed the mechanoresponsive self-growing hydrogels based on Double Network hydrogel system.[2] This synthetic hydrogel successfully mimic the muscle building behavior through cycling stretching in monomer solution. This self-enhancing hydrogel is prospective in emerging areas like soft-robotic and tissue-engineering. But the big disadvantage of this system is that you have to incorporate the toxic monomer solution in the hydrogel, and strict environment for training will also limit the practical application.

Hence, in this chapter, we focus on the biopolymer system. Unlike synthetic polymer system, there is no need for monomer solution, we will take fully advantage of the physiochemical property of the biopolymer to explore the self-enhancement behavior.

Previously, we successfully developed a simple method which named Drying in Confined Condition method, simple as DCC method. By using DCC method, we successfully improved the mechanical performance of alginate and cellulose hydrogel. The mechanical property of those DCC hydrogels reached the same level of connective tissues in human body like tendon and ligament. And we confirmed the biomimetic fibrous structure in those hydrogels. It would be very reasonable to ask is it possible to further improve the mechanical performance of those hydrogel. Or in other words, has the cellulose hydrogel or alginate hydrogel already fully adapted to the DCC method, is there still potential for further improvement?

In this chapter, we will train the cellulose hydrogel through repetitive DCC method, as shown in Figure 6.1, and try to explore the mechanical limit of cellulose hydrogel. And it has been shown that repetitive DCC method can effectively improve the mechanical property of DCC-Cellulose, despite their high strength. Some simple characterization has also been tried to find the origin of this self-enhancement behavior.

6.2 Experimental

6.2.1 Materials

Cellulose source (Advantec filter paper, Toyo Roshi Kaisha Ltd., Japan), DMAc and lithium chloride (Tokyo Chemical Industry Co., Ltd, Japan), acetone (Kanto Chemical Co., Inc.,

Japan), and ethanol (Imazu Chemical Co., Ltd.) were used as received without further purification. All the aqueous solutions were prepared using ultrapure deionized water.

6.2.2 Gels preparation

Cellulose hydrogels were prepared from filter papers, as previously reported, with some minor difference.9 The cut filter paper sheets were sequentially washed with water and ethanol. The washed paper was then activated by immersion in DMAc for 12 h and then vacuum dried at 60 °C. To prepare the cellulose solution, 0.75 g activated cellulose was dissolved in 100 g of LiCl/DMAc (8 g: 92 g). The cellulose solution was cast into a glass mold with a thickness of 3 mm. The solution was left in air under ambient conditions (temperature, 20 °C; humidity, 20%). After 2 days, the solution became a weak gel due to the diffusion of water molecules from the air into the cellulose solution. The weak cellulose gel was then placed in pure water and equilibrated for 2 days, changing the water every 12 h, to obtain the cellulose hydrogel (thickness ~2 mm). The cellulose hydrogels were cut into small pieces 10 mm wide, and 40 mm long and ~2 mm thick, and then loaded into the clamping devices with an initial length between the clamps of 30 mm, and then left drying under the air to record the force change during drying process. After the sample become totally dried, we take it off the clamp of tensile tester, and re-immerse the sample in water, and then after the equilibrium was reached, we got DCC-0%, and then repeat the above steps, we get DCC-0%, 0%. If we keep repeat the step for one more time, then we name the sample as DCC-0%, 0%x2, which means this cellulose hydrogel has been trained with DCC method for 3 times, and no prestrain has applied upon each training process. Above is the description

of naming rules for cellulose hydrogels, one more example for this rule, DCC-50%, 0%x2, this sample means the cellulose hydrogel has been trained first with 50% prestrain DCC process, and another 2 times 0% prestrain DCC process.

6.2.3 Mechanical tests

Mechanical properties. Tensile tests of gels were conducted in air at room temperature (25 °C) using a commercial mechanical tester (Instron 5965). The tensile speed was 100 mm/min. The distance between the clamps was fixed at 30 mm. Three specimens were used to test each sample. A cyclic loading-unloading test with a strain of up to 20% was also carried out in a moist environment to prevent water evaporation. The waiting time between the cycles of each test was 30 min. Stress was defined as the force divided by the initial cross-sectional area of the sample. The fracture stress and fracture strain were defined as the nominal stress and strain at the fracture point, respectively. The Young's modulus E was defined as the value of the initial slope of the stress–strain curve. Force change tests: Cellulose hydrogel was fixed on the tensile tester with initial length of 30 mm, and then left drying under the air to record the force change during drying process.

6.2.4 Structure characterization

Laser scan confocal microscope observation on the surface of fully died DCC samples. On the last step of DCC method, after the hydrogel has been dried for 12 hours on the DCC device, take it off for LSCM observation.

6.3 Results and Discussion

After the DCC samples were prepared under different prestrain, 0%, 50%, 100% respectively, then we fix the prestrain at 0%, to check how the DCC training will function on the morphology change of cellulose hydrogels. After first DCC process, we tried DCC process with 0% prestrain for another 4 times. As we can see in Figure 6.2, swelling ratio along width and thickness direction shows unstable change while length direction is very stable, however the training times are, there is no change in length direction. According to the swelling ratio results, we conclude there is no obvious morphology change in macrolevel.

And then we checked the force change during DCC training process, as shown in Figure 6.3, the force become stable since the second training process, however the prestrain in initial DCC training. This results seem to be a reflection of the fibrous structure become stable after first DCC training.

But in tensile tests, we surprisingly find that second DCC training has greatly improved the mechanical performance of cellulose hydrogel. As we can see in Figure 6.4, we summarized the change of fracture stress, fracture strain and young's modulus. And the DCC training are obviously more effective on cellulose hydrogel with higher prestrain DCC training, the DCC-100% shows a larger improvement in fracture stress after second DCC training compare with

other cellulose hydrogels. And there is no decline in fracture strain, which means one more DCC method has effectively improved both strength and toughness of cellulose hydrogels. And young's modulus shows no obvious change after repetitive DCC training.

Then we used Laser scanning confocal microscope to check the structure change after each DCC training process. As we can see in Figure 6.5, with more DCC training times, fibrous structure seems to become more aggregated together to form thick fibril bundles. As shown in Figure 6.6, more DCC training process makes the fibrils become more aggregated together, it reasonable to speculate that one time DCC training is not enough to make the fibrils fully aggregated together, the fibrous structure are very potential in forming thick fibril bundles to delay the devastating break of structure during stretching. This research still not finished yet, when cellulose hydrogel is trained by the same DCC process, they should reach a stable state, the fibrous structure will stop from forming thicker fibril bundles, and fracture stress will also touch a limits. In our future work, we will try to explore this limits.

But before that, we simply tried DCC training process with different prestrain, as shown in Figure 6.7, we use the limit training method to find the mechanical performance limits of cellulose hydrogels. After first DCC process with different prestrain, 0%, 50%, 100% respectively, in the second DCC training process, we push the DCC-0%, DCC-50%, DCC-100% to their limits strain, which is 100%, 50%, 20% respectively. And according to the results, the fracture stress of cellulose hydrogel is hard to breakthrough 90 MPa. Due to the limited samples, no further conclusion can be made, but without doubt, repetitive DCC process is a simple and effective method to improve the mechanical performance of cellulose

hydrogels. In the future, this training method will be applied on other biopolymer like alginate, collagen and so on.

6.4 Conclusion

By using DCC process as training method, we successfully further improved the mechanical property of cellulose hydrogel. By various characterization, we confirmed repetitive DCC process didn't change the size of cellulose hydrogel, but fibrous structure has been changed, cellulose fibrils become more aggregated together after each DCC process, the reason for this aggregation is not clear yet. But, however the aggregation mechanism is, the structure should eventually reach a equilibrium state when keep repeating the DCC process, and the limit of the mechanical property shall also be reached. By giving a extreme pretrain in the second DCC process, we find the fracture stress is hard to breakthrough 90 MPa, more experiments will be conducted for verification in the future.

6.5 References

[1] Wegst, U., Bai, H., Saiz, E. et al. Bioinspired structural materials. Nature Mater 14, 23–36 (2015). https://doi.org/10.1038/nmat4089

[2] Takahiro Matsuda, Runa Kawakami, Ryo Namba, Tasuku Nakajima, Jian Ping Gong, Mechanoresponsive self-growing hydrogels inspired by muscle training. 2019. 363. 6426. 504-508. DOI: 10.1126/science.aau9533

6.6 Figures

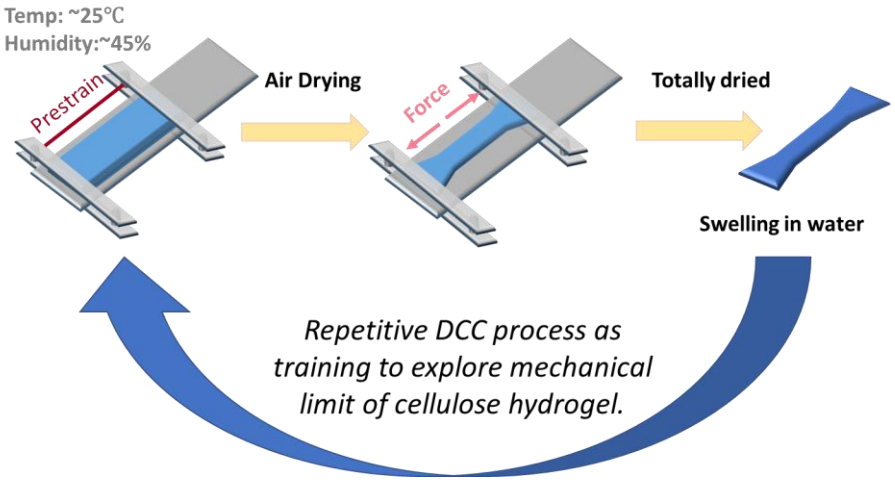

Figure 6.1 Schematic illustration of using DCC method as training method to cellulose hydrogel.

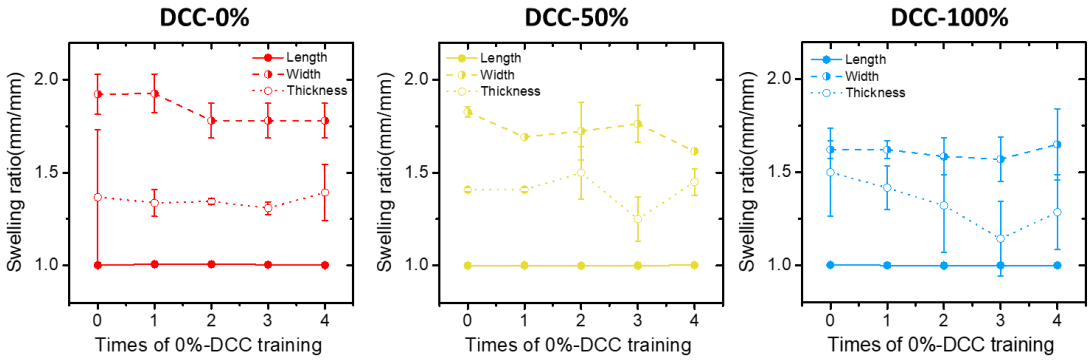

Figure 6.2 The change of swelling ratio of DCC samples along different direction after various training times.

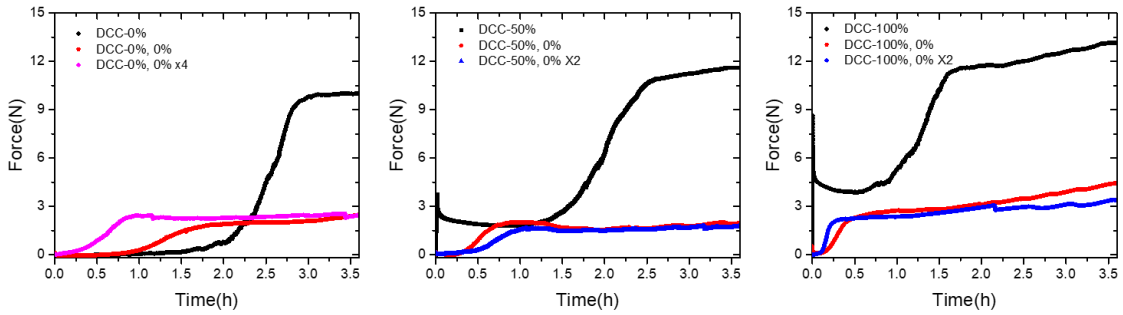

Figure 6.3 Force change during repetitive DCC process.

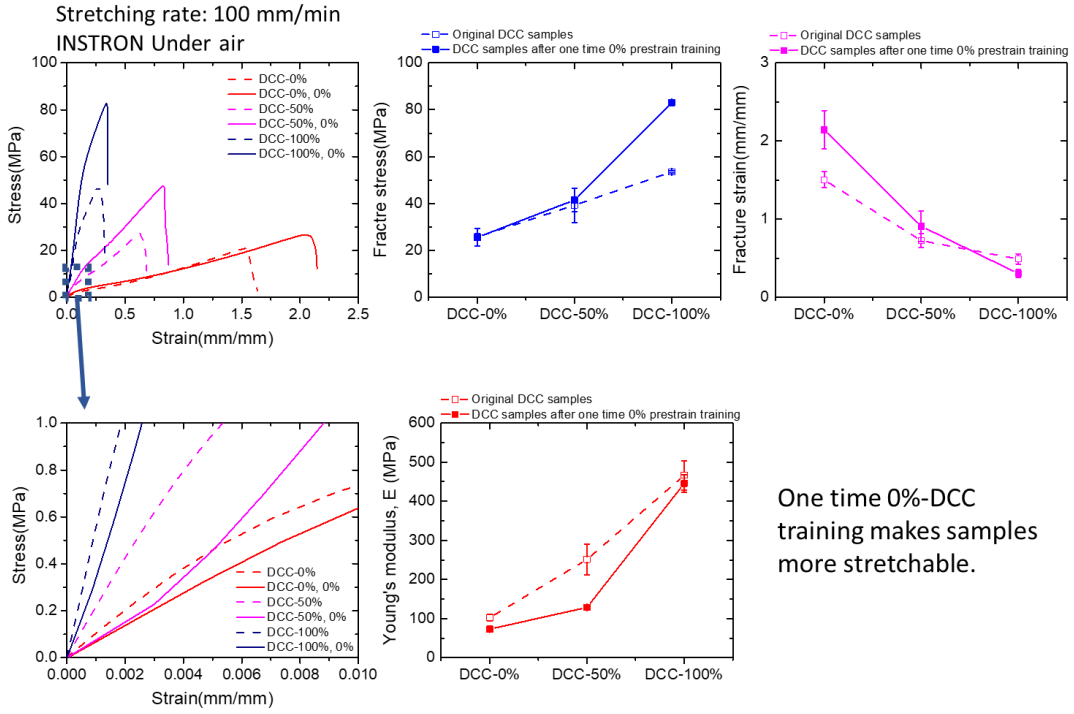

Figure 6.4 a. Tensile tests results of cellulose hydrogels after different DCC training method. b. fracture stress change after 2 times DCC training. c. Fracture strain change after 2 times DCC training. d. Young's modulus change after 2 times DCC training. e. Summary of the change of young's modulus.

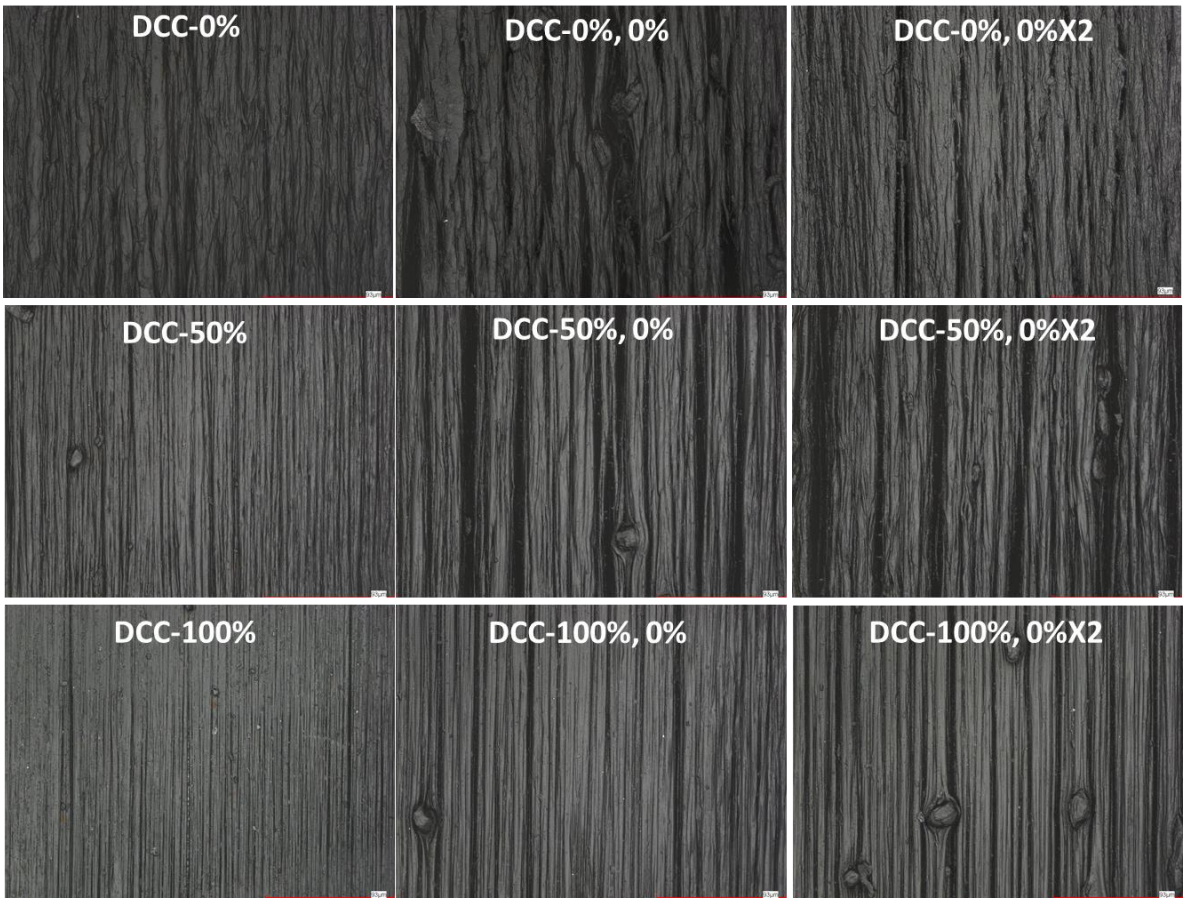

Figure 6.5 Laser scanning confocal microscope observation on the surface of cellulose hydrogels after multiple DCC training process.

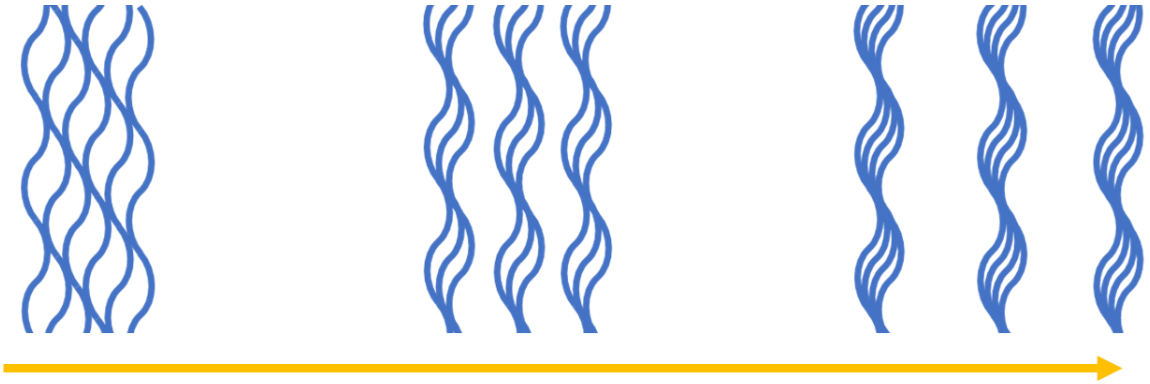

Figure 6.6 Schematic illustration of the change of fibrous structure after multiple DCC training.

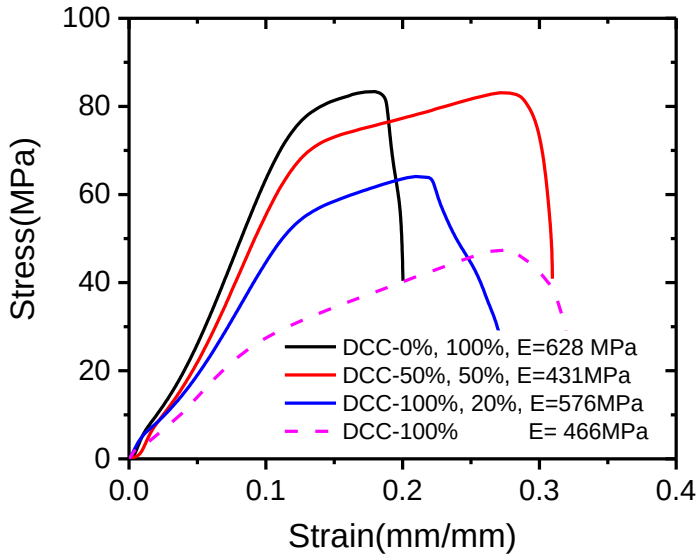

Figure 6.7 Comparison between cellulose hydrogels with different DCC training process.

CHAPTER 7

Conclusions

This dissertation proposed various ways to improve the mechanical property of cellulose hydrogels based on the facile method called Drying in Confined Condition method, simple as DCC method, and explored the structure origin of the excellent mechanical property with various characterization method. The method used to improve cellulose hydrogels is highly potential in improving the mechanical property of other biopolymer hydrogels. Conclusions of this dissertation are as follows.

In Chapter 3, by preparing original cellulose hydrogel under different humidity, we confirmed that 25℃ 20% humidity are the optimum conditions, because original cellulose hydrogel prepared under this environment show ideal shape, and stretchability. Then DCC method was applied to the original cellulose hydrogels under different temperature. High temperature will induce a fast crosslinking between fibrils, and resulted sample show a fibril bundles that not well separated. The process of aggregation of fibrils into fibril bundles need sufficient time space.

In Chapter 4, we successfully created DCC-E hydrogels, characterized by a Young's modulus and fracture stress close to the level of the Achilles tendon in the human body. The key is to use ethanol as the anti-solvent for the preparation of the original cellulose gels (alcogels) for the DCC process, which leads to sparser and straighter network strands of the cellulose alcogels compared to the cellulose hydrogels. The main reason for the significant

improvement in mechanical properties is attributed to be the higher degree of cellulose orientation observed in the DCC-E gels from the molecular scale to the submicron fibril scale. We confirmed this observation by hierarchical structural analyses using SEM, SAXS, and WAXD. Finally, this study provides a simple strategy to improve and modulate the mechanical performance of biopolymer materials by controlling the fibril arrangement, which could expand the application field of biopolymers to tissue engineering and soft electronics.

In Chapter 5, we confirmed the irreversible hysteresis and reversible hysteresis by cycling tests, and through quasi in situ SEM observation, we confirmed that the untwisting behavior of fibrous structure. Twisted area might contribute large amount of energy to total hysteresis, and most of which might be irreversible. Then, by doing cycling tests with different stretching rate, we found that cellulose samples show very limited viscoelasticity, and by fitting the results from irreversible hysteresis and reversible hysteresis we found that reversible hysteresis shows a larger viscoelasticity compare with irreversible hysteresis. And by using urea solution to undermine the hydrophobic interaction between cellulose fibrils we found that hydrophobic interaction plays an important role in both irreversible hysteresis and reversible hysteresis. Combine the SEM observation, we found that there could be 2 different kinds of cross-linking between cellulose fibrils, one is strong interaction which is hard to break though immersion in urea solution, another one is weak interaction which could be broken though urea solution, and make the cellulose fibrils separated. Quantify work need to be done to research interaction between fibrils, urea solution with different concentration will be used to further check the resulted change in mechanical performance.

In Chapter 6, by using DCC process as training method, we successfully further improved the mechanical property of cellulose hydrogel. By various characterization, we confirmed repetitive DCC process didn't change the size of cellulose hydrogel, but fibrous structure has been changed, cellulose fibrils become more aggregated together after each DCC process, the reason for this aggregation is not clear yet. But, however the aggregation mechanism is, the structure should eventually reach a equilibrium state when keep repeating the DCC process, and the limit of the mechanical property shall also be reached. By giving a extreme pretrain in the second DCC process, we find the fracture stress is hard to breakthrough 90 MPa, more experiments will be conducted for verification in the future.

Publications

(1) Yun Zhou Guo, Tasuku Nakajima, Md. Tariful Islam Mredha, Hong Lei Guo, Kunpeng Cui, Yong Zheng, Wei Cui, Takayuki Kurokawa, Jian Ping Gong, Facile Preparation of Cellulose Hydrogel with Achilles Tendon-like Super Strength through Aligning Hierarchical Fibrous Structure. Chemical Engineering Journal. 2021. Accepted

(2) Md. Tariful Islam Mredha, Yun Zhou Guo, Takayuki Nonoyama, Tasuku Nakajima, Takayuki Kurokawa, Jian Ping Gong. A Facile Method to Fabricate Anisotropic Hydrogels with Perfectly Aligned Hierarchical Fibrous Structures. Advanced Materials. 2018, 1704937, DOI: 10.1002/adma.201704937

(3) Wei Cui, Daniel R. King, Yiwan Huang, Liang Chen, Tao Lin Sun, Yun Zhou Guo, Yoshiyuki Saruwatari, Cung-Yuen Hui, Takayuki Kurokawa, Jian Ping Gong. Fiber-

Reinforced Viscoelastomers Show Extraordinary Crack Resistance That Exceeds Metals. Advanced Materials, 32(31), 1907180 (9 pages) (2020)

(4) Yong Zheng, Ryuji Kiyama, Takahiro Matsuda, Kunpeng Cui, Xueyu Li, Wei Cui, Yun Zhou Guo, Tasuku Nakajima, Takayuki Kurokawa, Jian Ping Gong. Nanophase Separation in Immiscible Double Network Elastomers Induces Synergetic Strengthening, Toughening, and Fatigue Resistance. Chemistry of Materials, 33(9), 3321-3334 (2021)

Presentations

(1) YunZhou Guo, Md. Tariful Islam Mredha, Tasuku Nakajima, Takayuki Kurokawa, Jian Ping Gong, "Controlling hierarchical fibrous structure of cellulose hydrogel", 67th SPSJ Annual meeting, Nagoya, 20180523, Presentation.

(2) YunZhou Guo, Md. Tariful Islam Mredha, Tasuku Nakajima, Takayuki Kurokawa, Jian Ping Gong, "Anisotropic toughness of DCC-Cellulose hydrogel with a highly aligned fibrous structure", 68th SPSJ Annual meeting, Sapporo, 20180923, Presentation.

(3) YunZhou Guo, Md. Tariful Islam Mredha, Tasuku Nakajima, Takayuki Kurokawa, Jian Ping Gong, "Anisotropic toughness of DCC-Cellulose hydrogel with a highly aligned fibrous structure", The 12th SPSJ International Conference, Hiroshima, 20181205, Presentation.

Acknowledgements

First I would like to give my great thank to Gong sensei for offering me the opportunity to study in LSW, and giving me patient instruction during my PhD courses. The deep professional knowledge, the high standard in research and persistent spirit of Gong sensei have given me the best science lesson and will drive me to do my work in a similar manner in the future.

Second, I want to give special thanks to Nakajima sensei, for always being patient when giving me research suggestions. Especially in last year, Nakajima sensei took a lot of efforts in revising my paper in his extremely busy time. The help from Nakajima sensei means a lot to me and my family during pandemic.

Then I would like to thank Dr. Guo HongLei and Dr Tarif, for giving me specific instructions in doing experiments and designing the research. Dr. Guo HongLei always gives fast response and patient help whenever I met the problem. Dr. Tarif is also so kind in sharing his knowledge with me without any hiding. The help from Dr. Guo and Dr. Tarif are so important when I first entered LSW.

Next, I would like to thank Cui sensei, Sun sensei, Dan sensei, Nonoyama sensei and Kurokawa sensei for their help in my research. Especially Cui sensei, for his kind instruction in my analysis in the X-ray data.

Special thank also need to give to secretaries, Hasegawa san, Iseya san for their assistance in preparing the documents and arranging the schedules.

And I also want to thank Zheng Yong san, Cui wei san, Martin san, Li Xueyu san, Yu ChengTao san, Wang Zhijian san, Fukao san, Kiyama san, Okumura san, Tanaka san and many other students and stuffs of LSW, it's nice to meet you all in Sapporo. Looking forward to meet you again if possible.

I also sincerely thank the IGP (international Graduate Program) and CSC scholarship for financial support during my PhD study.

Being a PhD student here in LSW and in Sapporo is my great luck, the atmosphere and the solid knowledge of all the Professors, staffs and students are so impressive to me. Five years' study here has profoundly changed me, all the discussion and cooperation with LSW members helped me to accumulate the knowledge from different areas, and most importantly, I've learned how to do a systematic research and thinking in a scientific pattern through long term accumulation. Those precious experience will definitely help me build a better career in my future work. And I feel pitiful that I didn't spend more time on research, my understanding in polymer science is still superficial, there are still so much could be leaned.

In the last, I want to thank my parents for supporting me through so many years, and I would like to thank my wife HanYang, she's also a PhD student in LSW, and she sacrificed so much for me and our son. Thanks for giving me support in the most difficult time during pandemic, and thanks for taking excellent care of our son, you are the light of my life, hope to see you and our son come back safely in HangZhou. Bright new life is ahead.

Guo, YunZhou

Laboratory of Soft & Wet Matter

Graduate School of Life Science

Hokkaido University

Sapporo, Japan